

Artificial Intelligence and Multiscale Modeling for Sustainable Biopolymers and Bioinspired Materials

Xing Quan Wang, Zeqing Jin, Dharneedar Ravichandran, and Grace X. Gu*

Biopolymers and bioinspired materials contribute to the construction of intricate hierarchical structures that exhibit advanced properties. The remarkable toughness and damage tolerance of such multilevel materials are conferred through the hierarchical assembly of their multiscale (i.e., atomistic to macroscale) components and architectures. Here, the functionality and mechanisms of biopolymers and bio-inspired materials at multilevel scales are explored and summarized, focusing on biopolymer nanofibril configurations, biocompatible synthetic biopolymers, and bio-inspired composites. Their modeling methods with theoretical basis at multiple lengths and time scales are reviewed for biopolymer applications. Additionally, the exploration of artificial intelligence-powered methodologies is emphasized to realize improvements in these biopolymers from functionality, biodegradability, and sustainability to their characterization, fabrication process, and superior designs. Ultimately, a promising future for these versatile materials in the manufacturing of advanced materials across wider applications and greater lifecycle impacts is foreseen.

1. Introduction

Every living being is a masterpiece of nature, intricately crafted with biopolymers whose precise multiscale hierarchical structures energize bio-inspired composites. Biopolymers can be classified into natural biopolymers and synthetic biopolymers. Natural biopolymers are the polymers produced by living organisms, such as proteins and polysaccharides. Biopolymer nanofibrils (e.g., cellulose, chitin, silk) are the typical natural biopolymers that spur innovation and interest due to their remarkable hierarchical structural features and functional outcomes, along with their green origins.^[1-3] The sophisticated hierarchical structure of biopolymer nanofibrils, spanning from the molecular to nano and macroscopic scales, features well-organized structural elements interconnected by extensive hydrogen bonding networks within semicrystalline matrices at each level. This intricate arrangement provides biopolymer nanofibrils with remarkable

mechanical stability and strength. Similarly, synthetic biopolymers can also possess a hierarchical structure, depending on the specifics of their design and synthesis processes. Many synthetic biopolymers are designed to mimic the natural hierarchical structures found in biological systems, often leading to enhanced properties similar to their natural counterparts.^[4,5] By engineering synthetic biopolymers with hierarchical features, researchers can replicate some of the remarkable properties of natural materials, such as toughness, elasticity, or self-healing capabilities.^[6,7] For instance, biodegradable polyesters can be synthesized and processed to form structures with hierarchical features, such as crystallites at the nanoscale and fibrous assemblies at larger scales, leading to improved strength and biodegradability. Synthetic collagen has a distinct hierarchical arrangement, synthetic versions can be designed to self-assemble into fibrils or higher-order structures to achieve similar mechanical properties. Bioinspired composites are designed based on principles observed in natural systems, which incorporate both synthetic and natural components for replicating their multiscale hierarchical structures and functionalities.^[8,9] Sustainable biopolymers and bioinspired materials are engineered to minimize environmental impact throughout their lifecycle by leveraging biodegradability, recyclability, or compostability, making them essential for addressing pressing challenges such as reducing persistent microplastics, mitigating greenhouse gas emissions, and improving resource efficiency within circular economy frameworks. A deep understanding of how natural systems organize matter, from the atomic to the macroscopic scale, is pivotal not only for appreciating the intrinsic properties of biopolymers but also for informing the synthesis of new and sustainable materials.

Computational and theoretical models provide essential tools for designing and optimizing biopolymer-based systems. Capturing the multiscale phenomena inherent to these materials requires multiscale approaches that span broad temporal and spatial resolutions. Multiscale modeling techniques in biopolymer and bio-inspired design differ primarily in how they integrate microscopic details into the macroscopic scale.^[10] Based on these differences, multiscale modeling approaches are categorized as hierarchical and concurrent methods.^[11] Hierarchical methods decompose a problem into multiple levels based on temporal or spatial scales, with information flowing from fine-scale to

X. Q. Wang, Z. Jin, D. Ravichandran, G. X. Gu
Department of Mechanical Engineering
University of California Berkeley
Berkeley, CA 94709, USA
E-mail: ggu@berkeley.edu

 The ORCID identification number(s) for the author(s) of this article can be found under <https://doi.org/10.1002/adma.202416901>

DOI: [10.1002/adma.202416901](https://doi.org/10.1002/adma.202416901)

macroscopic through step-by-step analysis, allowing specialized techniques to be applied at each level. In contrast, concurrent methods, address multiple scales simultaneously within a single computational domain, integrating different scales, and using mathematical relationships for real-time interaction and scale coupling. Multiscale modeling for biopolymers primarily relies on hierarchical methods rather than concurrent methods due to the complex, scale-dependent nature of biopolymer structures and their properties.^[12,13] For biopolymers and biological processes, the typical length scales range from the ångström-level interactions of individual chemical bonds to the interactions at the level of monomers and single polymer chains, extending to the formation of specific domains and more complex 3D structures unique to these systems. This hierarchical organization is evident not only in the crystalline regions and blending characteristics of polymer mixtures and composites, but also in the higher-order assembly of proteins and polysaccharides, which provide additional contributions to the formation of macroscopic structures in biopolymers. Consequently, hierarchical methods are particularly well-suited for such systems, as they allow the problem to be decomposed across different scales, facilitating the optimization of material structures at each level according to the performance requirements associated with the relevant scale. Furthermore, hierarchical approaches offer greater computational efficiency in modeling biopolymers by simultaneously simulating multiple scales within a single computational domain.^[14] These methods enable the progressive upscaling of information from the atomistic to the macroscopic level, making them more practical for capturing the full complexity of biopolymer systems while maintaining both precision and computational feasibility. When combined with experimental validation techniques such as 3D printing,^[15–20] multiscale methods allow for precise control over hierarchical structures in synthetic biopolymers, enhancing key material properties such as mechanical strength, porosity, and biodegradability.

Integrating artificial intelligence (AI) into the design of biopolymers and bio-inspired composites offers a promising approach to advancing sustainability in materials science.^[21–24] AI, particularly through machine learning (ML) algorithms, excels at processing and analyzing large datasets, which include molecular structures, processing conditions, and environmental impacts.^[25–29] By uncovering complex patterns and relationships within these datasets, AI facilitates accurate predictions of material properties and performance, significantly reducing the need for extensive experimental trials. In ML-driven biopolymer design, ML models are typically categorized into three types based on their outputs: regression models, which provide continuous numerical predictions; classification models, which assign inputs to distinct categories; and clustering models, which group data points based on shared features without supervision.^[30] These models often use design parameters as input features, enabling the prediction of critical mechanical and chemical properties such as strength, deformation, toxicity, stiffness, and stability. This predictive capability accelerates the discovery of new biopolymers with optimized traits, such as improved biodegradability, mechanical strength, and thermal stability, reducing both resource consumption and waste. Generative models form a distinct class of algorithms focused on learning from data to create new samples or design novel objects, rather than simply predict-

ing or classifying.^[31] In the context of bio-inspired composites, generative models like generative adversarial networks (GANs) and variational autoencoders (VAEs) can generate novel microarchitectures that mimic natural hierarchical patterns, producing materials with superior mechanical properties and reduced environmental impacts. Transformers, the foundational architecture of large language models (LLMs), employ a self-attention mechanism to capture global relationships within input data, including both text and images. This flexibility has made Transformers one of the most widely adopted deep learning frameworks. In biopolymer research, Transformers are expected to be applied in analyzing material life cycles by evaluating factors such as energy consumption, carbon emissions, and recyclability. These comprehensive analyses support the development of biopolymers that are both functional and sustainable across their entire lifespan. AI also plays a key role in bridging the gap between laboratory discoveries and industrial production by optimizing manufacturing processes such as 3D printing parameters and self-assembly techniques.^[32–35] This approach helps identify optimal processing conditions, reducing energy consumption and material waste while enhancing overall material performance.

This review presents a multiscale perspective on AI-enhanced sustainable biopolymers and bioinspired design. We begin with a comprehensive overview of the multiscale architectures of biopolymers, introducing the progression from simple to hierarchical to complex configurations in both natural and synthetic biopolymers, as well as sustainable copolymers for hierarchy development in bio-composites. Next, we explore multiscale modeling approaches for biopolymers, covering both particle-based and field-based methods, along with experimental validation techniques. We then highlight how AI can be leveraged for characterization, fabrication optimization, and generative design of advanced biopolymers. Finally, we conclude with an outlook on future developments in the field.

2. Multiscale Architectures of Biopolymer: Simple-Hierarchical-Complex Configurations

The architecture of polymers refers to the specific arrangement and connectivity of polymer chains, which significantly influences their physical, thermal, and chemical properties.^[36] Natural biopolymers like proteins, nucleic acids, and polysaccharides exhibit highly complex hierarchical architectures that span from individual monomers to large macroscopic assemblies.^[37] This complexity is the result of millions of years of evolution fine-tuning them for specific biological roles. In contrast, synthetic biopolymers engineered by humans have simpler architectures but offer precise control, allowing customization for specific industrial or scientific applications.^[38] A key difference between natural and synthetic biopolymers lies in their inherent complexity and composition: natural biopolymers have intricate, specialized architectures optimized for biological performance, while synthetic biopolymers provide greater design flexibility for tailored uses. Table 1 underscores this contrast by highlighting the complexity of natural biopolymers and the versatility of synthetic ones.^[8,39–41] While nature's biopolymers perform essential biological functions precisely, synthetic biopolymers are adaptable and valuable across fields like medicine, material science, and engineering.

Table 1. Comparison of natural and synthetic biopolymers highlighting the key differences in their architecture.

	Natural Biopolymers	Synthetic Biopolymers
Structure	Exhibits complex, multilevel organization.	Exhibits a more uniform and less complex architecture.
Composition	Monomers are arranged in precise, biologically determined sequences providing unique folding and functions.	Engineering monomer sequence giving tailored properties and functionalities.
Conformations	Can form helices, sheets, and complex 3D structures often stabilized by hydrogen bonding and other interactions.	It can be linear, branched, star-shaped, or form networks providing specific applications.
Versatility	Can self-assemble spontaneously and organize into higher-order structures.	Can produce hydride structures through a combination of synthetic and natural components.
Dispersity	These are monodispersed, i.e., all molecules have the same mass and composition.	Often polydisperse with a distribution of masses.
Hierarchy	Exhibit multiple levels of hierarchical organization from primary to quaternary or individual units to branched structures	Generally, lacks the complex hierarchical organization.
Functionality	Produces highly specific and complex biological functions.	Can be designed for specific functions.
Biodegradability	Many natural polymers are inherently biodegradable.	Not all synthetic polymers are biodegradable but are biocompatible.

2.1. Natural Biopolymers

Natural biopolymers, derived from living organisms such as plants, animals, and microorganisms, are regarded as environmentally sustainable due to their natural origin, biocompatibility, and biodegradability.^[42] Natural biopolymers such as cellulose produced by plants contribute to environmental sustainability by sequestering up to 2–3 gigatons of carbon annually, which helps reduce atmospheric CO₂ levels.^[43] Their biodegradability under natural conditions ensures minimal environmental persistence, as materials like chitosan decompose within weeks to months in soil or aquatic systems and significantly reduce waste accumulation.^[44] Their eco-friendly nature and inherent biological properties have led to widespread use in various applications, especially in fields that prioritize sustainability and health. Based on their repeating structural units, natural biopolymers can be classified into three main categories: polynucleotides (e.g., DNA and RNA), polypeptides (e.g., proteins or protein-based biopolymers like gelatin), and polysaccharides (e.g., chitosan). All natural biopolymers exhibit a multiscale hierarchical architecture that allows them to display complex behaviors and functions across different length scales, playing a crucial role in determining the properties and capabilities of biological systems.^[45] At the nanoscale level, individual monomers form the basic building blocks. The monomer assembly into a polymer chain forms the secondary structure. The polymer chains are further organized into tertiary and quaternary structures, and on larger scales, they assemble into networks, fibers, and macroscopic structures. The structural organization varies among biopolymer types: polypeptides have a complex, well-defined four-level structure with amino acids forming primary sequences, secondary structures like alpha helices or beta sheets, tertiary structures as the overall 3D shape of a single protein molecule, and quaternary structures as assemblies of multiple protein subunits; polysaccharides have a simpler organization with primary structures of monomer sequences and linkage types, secondary structures of local chain conformations, and higher-order assemblies that are not as well-defined or universal as in polypeptides, although some exhibit multiscale hierarchical structures similar

to proteins.^[46,47] This hierarchical organization is determined by factors such as the chemical properties of the monomers, the types of bonds that link them, and the specific biological roles of the biopolymer. While polynucleotides are essential for numerous applications, they fall outside the scope of this review and will not be discussed much further.

2.1.1. Polypeptides

The hierarchical structure of polypeptides involves several levels of organization, from the primary amino acid sequence to intricate 3D architectures. This complexity arises through cooperative self-assembly processes, where higher-order structures are stabilized by interactions like hydrogen bonding and π - π stacking.^[48] These interactions enhance both the stability and complexity of the resulting structures. For long-range, ordered crystalline formations, self-assembly is governed by thermodynamic principles that dictate how polypeptides organize into specific forms. Unlike traditional crystallization mechanisms, hierarchical self-assembly employs a multiscale approach that coordinates both the structure and function of the material.^[49] This process leads to diverse architectures such as nanofibers, twisted nanoribbons, and nanotubes, depending on the sequence interactions between polypeptide chains. The chemical functionalities of the polypeptides and their interactions with other polymers play crucial roles in directing self-assembly into complex, stable structures, which are widely used in applications like biomaterials for cell culture scaffolds.^[50] The hierarchical organization of polypeptides is characterized by multiple levels of structural complexity (Figure 1A). The primary structure is the linear sequence of amino acids connected by peptide bonds, serving as the foundation for the polypeptide's overall shape and function. Each amino acid has a unique side chain, or R-group, which influences how the polypeptide folds and interacts with other molecules. The secondary structure refers to the local spatial arrangement of the polypeptide chain, resulting in common motifs like alpha helices and beta sheets stabilized by hydrogen bonds between backbone atoms.^[51] The tertiary structure

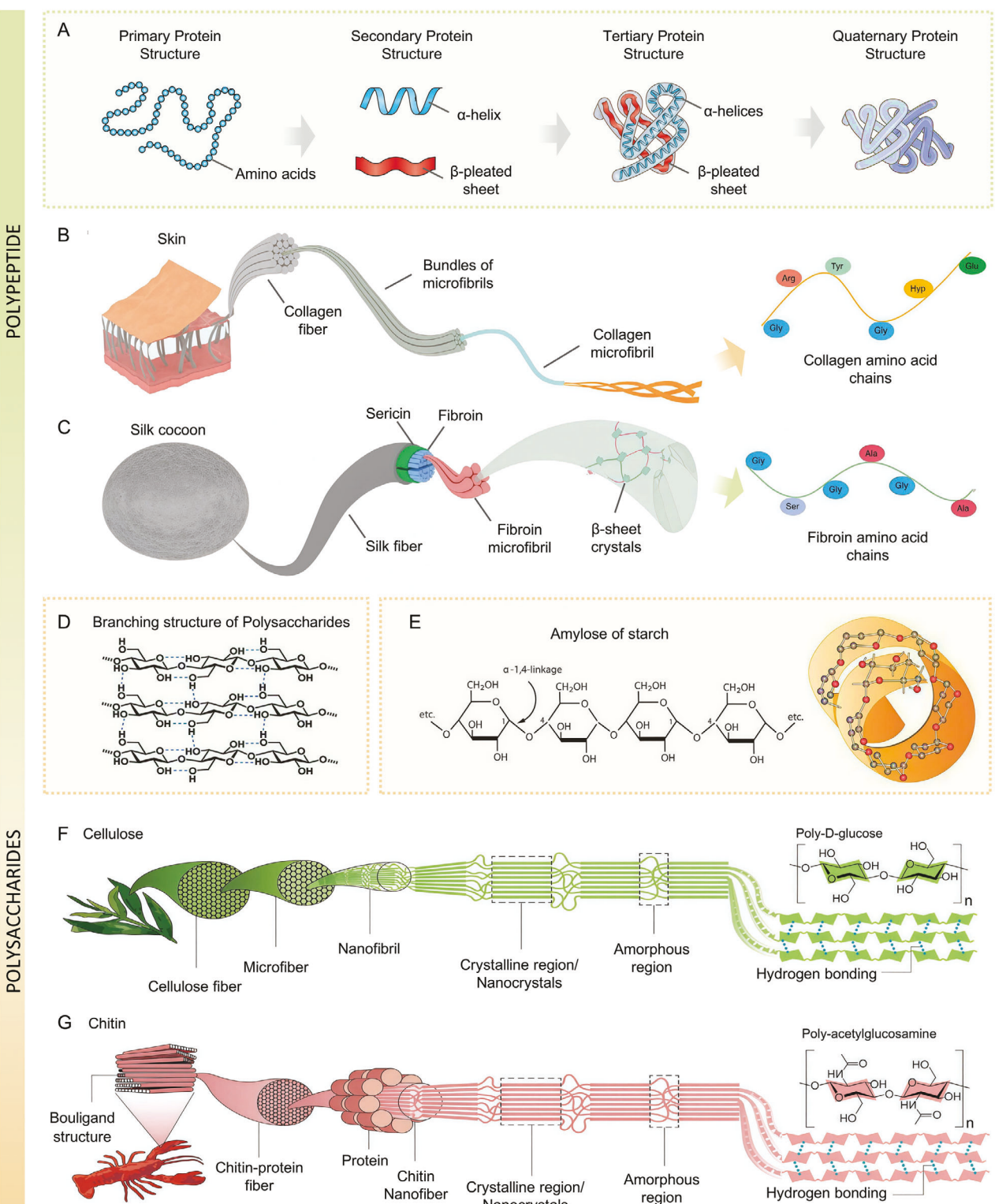


Figure 1. Hierarchical architecture of A–C) polypeptides and D–G) polysaccharides: A) the fundamental organization of polypeptides; Adapted with permission.^[28] Copyright 2024, OpenStax B) the hierarchy of collagen; C) The hierarchy of silk fibroin; Adapted with permission.^[64] Copyright 2023, MDPI. D) the fundamental branching structure of polysaccharides; Adapted with permission.^[67] Copyright 2020, RSC. E) molecular diagram of amylose of starch and a 3D illustration of the spiral amylose structure containing six glucose units per turn due to the hydrogen bonding; Adapted with permission.^[282] Copyright 2024, OpenStax. F) the hierarchy of cellulose. G) the hierarchy of chitin extracted from crawfish, highlighting the multilevel organization that enhances its properties and versatility. Adapted with permission.^[80] Copyright 2021, Wiley.

describes the overall 3D shape of a single polypeptide molecule, influenced by interactions between side chains, including disulfide bonds, hydrophobic interactions, hydrogen bonds, and ionic interactions.^[52] Some polypeptides exhibit a quaternary structure by forming larger functional complexes with other polypeptide chains.^[53] This level involves interactions of multiple subunits held together by noncovalent bonds and sometimes stabilized by disulfide bridges, critical for the function of many multisubunit proteins like hemoglobin. The hierarchical structure of polypeptides is inherently dynamic, with different levels exhibiting distinct timescales of motion. Rapid local fluctuations, such as side chain movements, occur within the pico- to nanosecond range. Motions of secondary structure elements like alpha helices and beta sheets happen over nano- to microsecond timescales. Larger-scale movements, including rearrangements of entire domains or subunits, span from microseconds to milliseconds. These dynamic movements are crucial for polypeptide functions, enabling processes like enzyme catalysis, ligand binding, and allosteric regulation.^[54–56] Understanding these hierarchical and dynamic properties is key to exploring their roles in biological systems, from enzymatic activity to molecular recognition, and provides a basis for innovations in biomaterials and protein engineering. By manipulating these structural hierarchies, researchers can develop new biomaterials and drugs with targeted functionality.

Collagen and silk are the typical natural biopolymers with hierarchical structures that provide mechanical strength, bioactivity, and suitability for biomedical applications. Collagen, the most abundant protein in the human body, exemplifies the helical structure in polypeptides and possesses a complex hierarchical organization crucial for its biological functions and tissue engineering applications.^[57] Beginning with amino acid chains forming its primary structure, collagen progresses from molecular triple helices to microfibrils, fibril bundles, and macroscopic fibers.^[58] This multiscale architecture enhances its mechanical properties like strength and toughness, making it suitable for load-bearing applications.^[59] The rigid, rod-like triple helices contribute to stability and functionality (Figure 1B), while the D-periodic cross-striated pattern of microfibrils adds mechanical strength.^[60] Collagen's structure also supports cell attachment, growth, and differentiation, making it an ideal scaffold for tissue regeneration.^[61] Silk, a natural polymer composed of fibroin, exemplifies the β -sheet structure in polypeptides and has been used in medical applications like surgical sutures.^[62] Silk fibroin, constituting about 70% of silk, possesses favorable properties such as strong mechanical performance, hydrophilicity, and biocompatibility.^[63] Its unique structural characteristics and hierarchical organization are crucial for tissue engineering and biomaterials (Figure 1C).^[64] Similar to collagen, silk fibroin exhibits a multilevel structure from molecular arrangements to macroscopic scaffolds.^[65] At the primary level, silk consists of two main proteins: fibroin and sericin. Fibroin is composed of a heavy chain (H-chain) and a light chain (L-chain) linked by disulfide bonds; the H-chain, rich in glycine, alanine, and serine, forms stable structural units. At the secondary level, the H-chain folds into stable anti-parallel β -sheets, providing strength and rigidity. These β -sheets aggregate to form tropo-silk, the fundamental building block of silk fibers. Tropo-silk aggregates align into fibrils, which bundle into fibers ranging from 10 to 30 microns in diameter, offering exceptional tensile strength and elasticity. At

the macroscopic level, these fibers are organized into larger structures that can be processed into films, scaffolds, or threads.^[62,63] This hierarchical organization allows silk fibroin to mimic the natural extracellular matrix, providing an ideal environment for cell adhesion and growth.^[66] Understanding and replicating the natural hierarchies of collagen and silk are crucial for developing advanced materials with enhanced performance and biocompatibility, particularly in regenerative medicine, surgical sutures, and other biomedical applications.

2.1.2. Polysaccharides

Unlike polypeptides, which have a well-established understanding of their multiscale molecular architecture, polysaccharides are less comprehended at the molecular level. This is due to challenges such as the lack of pure materials, difficulty in synthesis, and their branched structures (Figure 1D).^[67] Isolating polysaccharides from natural sources requires extensive purification and harsh treatments, often leading to polydisperse samples. However, polysaccharides exhibit a multilevel hierarchy, from basic monosaccharide units to complex supramolecular architectures. This hierarchy, including constituent sugars, branching patterns, macromolecular architecture, and supramolecular organization, plays a crucial role in determining their functionality and properties.^[46] At the primary level, polysaccharides are composed of monosaccharide units linked by glycosidic bonds, forming either homopolysaccharides or heteropolysaccharides. The primary structure involves glycosidic linkages in α or β configurations at different carbon positions. The secondary structure refers to the spatial arrangement influenced by hydrogen bonding and linkage types, resulting in helices (e.g., amylose) or ribbon-like structures (e.g., cellulose). At the tertiary and quaternary levels, polysaccharides form more complex 3D shapes, either as single molecules or as networks that interact with other biomolecules.^[68–70] These higher-order structures are affected by intramolecular interactions, branching patterns, and external factors such as pH, temperature, and ionic strength. Therefore, understanding this hierarchical organization is essential for appreciating their diverse functions and roles in biological systems.^[71–73] Despite being abundant in food, the literature on key polysaccharides like starch and alginate is incomplete due to structural complexity and analytical limitations.^[67] Nevertheless, their hierarchical structure is fundamental to their functional properties and applications in fields such as food science, drug delivery, and tissue engineering.

Starch is a polysaccharide composed of amylose and amylopectin, featuring a layered architecture that affects its solubility, digestibility, and industrial performance. Amylose, making up about 35% of natural starches, is a linear chain of glucose molecules.^[74] Its unbranched structure forms helical arrangements, influencing the starch's ability to gelatinize and resist enzymatic breakdown (Figure 1E). In contrast, amylopectin is the branched component with glucose units organized into clusters. This branching creates a dense network that affects how starch interacts with water, making it ideal for thickening agents, adhesives, and biodegradable materials.^[75] The biodegradability of amylopectin lies in its glucose-based structure, which can be enzymatically hydrolyzed by amylase and other naturally

occurring enzymes into simple sugars that microorganisms can easily metabolize. Studies have demonstrated that starch-based materials rich in amylopectin achieve over 50% biodegradation within weeks under composting conditions,^[76] highlighting their rapid and eco-friendly decomposition. The hierarchical arrangement of linear amylose interwoven with branched amylopectin determines starch's properties such as gelatinization temperature, viscosity, and resistance to digestion, which are crucial for its applications in food and industry.^[77] Similarly, alginate derived from brown seaweed is composed of blocks of mannuronic acid (M) and guluronic acid (G) arranged in a specific hierarchical structure. The alternating sequence of M and G blocks gives alginate unique properties, such as forming hydrogels in the presence of divalent cations like calcium.^[78] This hierarchical organization is essential for its use in applications such as drug delivery and tissue engineering. Alginate's gel-forming ability is harnessed to encapsulate cells, proteins, or drugs for controlled release.^[79] The hierarchical structures of both starch and alginate are critical for their interactions, stability, and functional properties.

Cellulose is an organic compound and the primary structural component of plants and algae, found in fruits, vegetables, and whole grains. Its complex hierarchical structure greatly influences its mechanical properties and wide range of applications (Figure 1F).^[80] At the molecular level, cellulose consists of repeating units of β -D-glucose connected by glycosidic bonds, forming long, linear chains.^[81] This straight-chain nature allows extensive hydrogen bonding between chains, which is crucial for stability. Each glucose unit contains hydroxyl ($-OH$) groups that enable these bonds, affecting cellulose's solubility and reactivity. At the fibrillar level, individual cellulose molecules aggregate to form microfibrils (i.e., bundles held together by hydrogen bonds). These microfibrils are typically 10 to 30 nm in diameter. They have crystalline regions that provide strength and rigidity and amorphous regions that offer flexibility and allow the material to absorb stress without breaking.^[82] Microfibrils further bundle into larger fibers ranging from 10 to 20 μ m in diameter that are organized to support plant cell walls. Fiber orientation varies based on function: parallel alignment withstands stretching forces, while random or patterned arrangements resist compression.^[83] Cellulose fibers are embedded in a matrix of hemicellulose, lignin, and other polysaccharides within the plant cell wall, forming a composite structure that provides both mechanical strength and flexibility.^[84] The plant cell wall is organized into three layers: an outer flexible layer for cell growth, a thicker inner layer for additional support, and a pectin-rich middle layer that acts as glue between adjacent cells.^[85] The hierarchical organization of cellulose from molecular structure to macroscopic arrangement is critical to its function as a biomaterial by providing mechanical strength and supporting essential biological processes.

Chitin ranks as the second most abundant polysaccharide following cellulose. It is a long-chain polymer comprised of N-acetylglucosamine units connected by glycosidic bonds. Found in the cell walls of fungi and the exoskeletons of insects and crustaceans, its hierarchical structure greatly influences its mechanical properties and applications (Figure 1G).^[80] At the molecular level, chitin's linear chains can self-assemble into organized matrices at multiple scales. These scales range from nanofib-

riils to macroscopic forms. Environmental factors like pH can trigger this self-assembly into nanofibrils.^[86] Techniques such as binary-solvent-induced self-assembly create chitin hydrogels with enhanced damping properties.^[87] Chitin exists in three polymorphic forms.^[87] α -chitin has antiparallel chains providing high stability. β -chitin has parallel chains found in marine organisms. γ -chitin is a combination of both forms. At the fibrillar level, chitin molecules form microfibrils which are bundles stabilized by hydrogen bonds. These microfibrils have diameters of 2 to 5 nanometers and lengths extending to several hundred nanometers. Crystalline regions contribute to mechanical strength. Amorphous regions provide flexibility.^[87] These microfibrils bundle into larger fibers 10 to 20 microns in diameter. These fibers are organized into layered structures that support biological systems. Chitin also forms cuticles, which provide the protective outer layer of organisms with a multilayered architecture composed of chitin composites.^[88] Fibers are arranged in a twisted, plywood-like structure, enhancing properties such as toughness and fracture resistance. This hierarchical organization makes chitin ideal for medical devices, biomimetic materials, and other engineering fields.^[89]

2.2. Biocompatible Synthetic Polymers to Biocomposites: Hierarchy Development

2.2.1. Synthetic Biopolymers and Synthesis

While natural biopolymers possess exceptional properties and functionalities, their extraction and processing often lead to significant performance deterioration including limited modifiability, poor solubility, and variability among batches.^[90] Considering these challenges, synthetic biopolymers have emerged as a promising alternative. Synthetic biopolymers, derived from renewable resources, offer cost-effective synthesis, tunable properties, and biodegradability, making them attractive for a wide range of applications in biomedical, pharmaceutical, and packaging industries.^[91] Unlike natural polymers, synthetic biopolymers can be tailored to meet specific requirements, allowing for greater control over their physical, chemical, and mechanical properties.^[92] The sustainability of a synthetic biopolymer depends on whether it is derived from renewable resources, biodegradable under natural or industrial conditions, and recyclable or upcyclable to support a circular economy. Its production should prioritize minimizing energy consumption and greenhouse gas emissions while ensuring nontoxicity to humans and ecosystems. Examples such as polylactic acid (PLA), polyvinyl alcohol (PVA), polyhydroxyalkanoates (PHAs), and polycaprolactone (PCL) demonstrate how functionality can be effectively combined with environmental responsibility. These sustainable synthetic polymers are widely used in applications such as drug delivery systems, tissue engineering, and 3D printing due to their biodegradability, biocompatibility, and favorable interaction with biological systems. Their ability to promote healing and regeneration, while minimizing adverse reactions, makes them particularly valuable in medical device manufacturing and tissue scaffolding.^[6]

Advancements in the fabrication methods have enabled the development of sustainable synthetic biopolymers, making them

Table 2. Key synthesize methods and examples of synthetic biopolymers.

Method	Technique	Description	Examples	Refs.
Polymerization	Coordination polymerization	Used to synthesize polyisoprenes, which are synthetic analogs of natural rubber. This method employs Ziegler-Natta catalysts to facilitate the polymerization process	Cis-1,4-polyisoprene, trans-1,4-polyisoprene	[277]
	Ring-opening metathesis polymerization	This technique allows for precise control over polymer structure, including side-chain placement, which is crucial for tailoring properties such as hydrophilicity and biocompatibility	Polynorbornene	[278]
Chemical	Polycondensation and polyaddition	These methods are commonly used to create PHAs and other biodegradable polymers. They involve the stepwise reaction of monomers to form high molecular-weight polymers	Poly(3-hydroxybutyrate), polyurethane, poly(hydroxovaleric acid)	[279]
	Esterification and hydrolysis	These reactions can modify existing biopolymers or synthesize new ones by linking monomers through ester bonds or breaking them down into simpler units	PVA, PCL, PLA, polyphosphazene	[279]
Chemoenzymatic	—	Enzyme-assisted synthesis utilizes specific enzymes to catalyze reactions, facilitating the formation of complex structures like polysaccharides and glycosaminoglycans. This approach can enhance specificity and yield in biopolymer production	PHAs, heparin, synthetic polysaccharides	[280]

ideal for specific biomedical applications. These polymers are synthesized through a range of chemical processes designed to replicate the beneficial properties of natural polymers while addressing their limitations. By refining the fabrication processes, researchers can fine-tune the structure and functionality of synthetic biopolymers to meet the demands of applications. Additionally, growing concerns over plastic pollution have increased interest in synthetic biopolymers as ecofriendly alternatives to conventional plastics, positioning them as essential contributors to achieving a more sustainable, carbon-neutral society.^[93] Table 2 provides an overview of major synthesis methods for sustainable synthetic biopolymers, along with a brief description of each process. While it is challenging to replicate the precise spatial configurations of natural polymers, synthetic polymers offer several advantages that could surpass natural counterparts. The cost-effective fabrication of synthetic polymers, combined with superior strength, durability, tunable properties, and consistent production, leads to greater processability and adaptability across various applications.

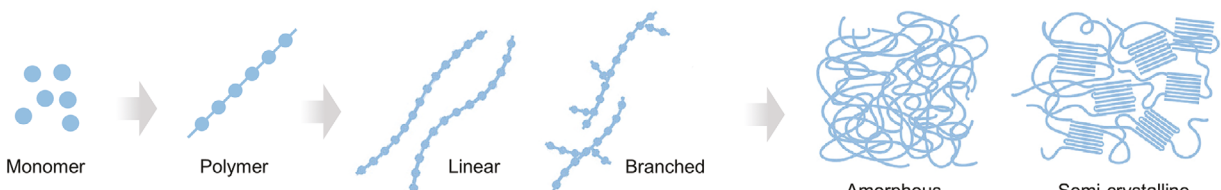
Moreover, unlike natural polymers, which inherently exhibit a hierarchical architecture, synthetic biopolymers also possess a hierarchical structure that can be described from the molecular to the macroscopic level (Figure 2A).^[80] They adhere to the classical definition of polymers, which are composed of repeating monomer units linked together through various polymerization processes. The primary structure is given by the arrangement of these monomers. At the nanoscale, synthetic biopolymers exhibit self-assembly into nanosized structures, where linear polymers can fold into cyclic forms, contributing to the formation of intricate hierarchical nanostructures. At the microscale, polymer chains can aggregate into larger domains through intermolecular interactions, influencing properties such as mechanical strength and thermal stability. At the macroscopic level, the bulk character-

istics of synthetic biopolymers such as shape, size, and mechanical performance become important for practical applications.^[38] For example, crosslinked polymers form networks that enhance durability and resistance to deformation, making them suitable for demanding real-world conditions. Specifically, the hierarchical architecture of synthetic biopolymers such as PHA, PVA, and PCL significantly influences their sustainability and functionality by regulating biodegradation rates, optimizing mechanical properties, enhancing processability, and enabling tailored molecular interactions. Studies have shown that the crystalline-to-amorphous ratio in PHAs affects enzymatic hydrolysis,^[94,95] while the interplay between crystalline and amorphous regions in PCL provides a balance of flexibility and durability.^[96,97] However, their relatively simple structural configurations limit their functionality compared to natural polymers. To address this, modifications to side groups or the main polymer chain can introduce greater complexity and mimic biological systems, enabling the development of more advanced materials. Through multiscale optimization, synthetic biopolymers can achieve application-specific performance by tailoring properties across molecular, microstructural, and macroscopic levels, minimizing material and energy use, reducing waste, and supporting sustainable end-of-life strategies such as recycling or controlled degradation.

2.2.2. Biocompatible and Sustainable Copolymer

Copolymers are intricate macromolecules created by polymerizing two or more different monomers, leading to diverse structures and properties. They can be categorized into several types, including random, alternating, block, graft, star, and hyperbranched copolymers, each offering unique molecular configurations and applications. Figure 2B-a illustrates various

A Structural configuration of synthetic polymers

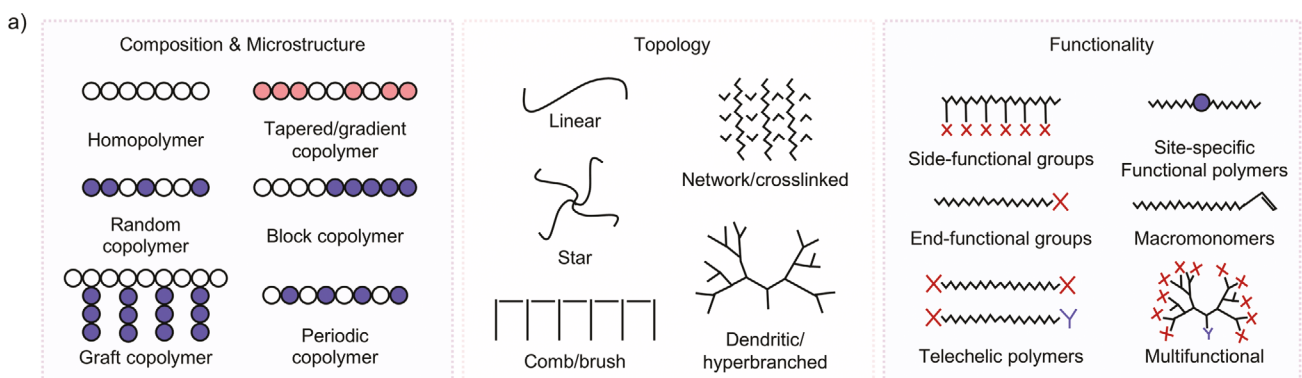


Molecular

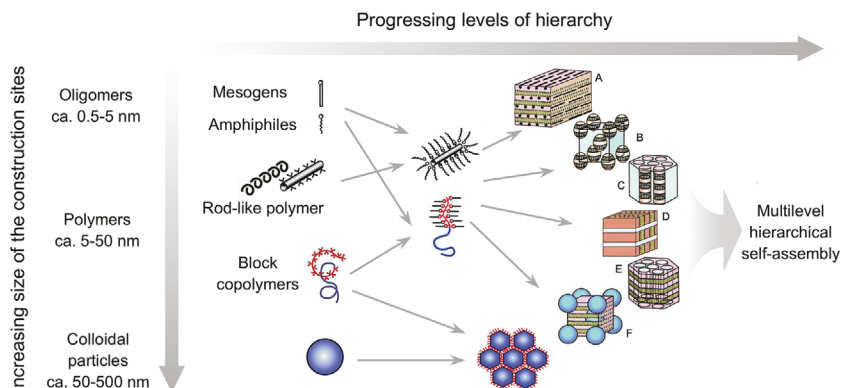
Nano

Micro

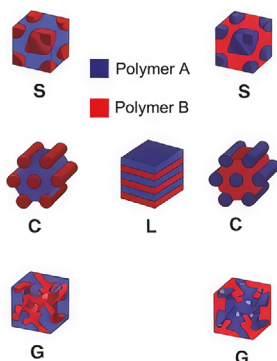
B Block copolymers – multifunctional biocomposites



b)



d)



c)

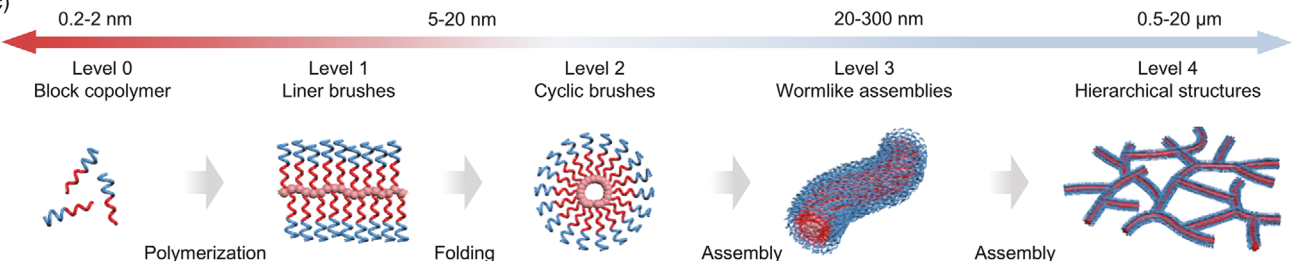


Figure 2. A) Illustration of the hierarchical structure of synthetic biopolymer chain assembly from molecular to microscale; Adapted with permission.^[80] Copyright 2021, Wiley. B) Self-assembly and the hierarchy of block copolymers a) composition, microstructure, topology, and functionality of copolymerization, Adapted with permission.^[98] Copyright 2005, Elsevier. b) highlights scenarios to construct hierarchically self-assembled polymeric structures with different sizes and lengths, Adapted with permission.^[99] Copyright 2004, RSC. c) a molecular dynamic simulation showing the self-assembly of cyclic brush copolymer, Adapted with permission.^[100] Copyright 2021, Springer Nature. d) illustration of various microstructures of self-assembled deblock copolymers. Adapted with permission.^[101] Copyright 2008, Elsevier.

molecular arrangements, topologies, and functional attributes of these copolymer types.^[98] Copolymers can be synthesized on different substrates to generate molecular structures that enable the controlled formation of nanostructured morphologies. As shown in Figure 2B-b, monomers of varying sizes can be combined to create a higher hierarchical structure, utilizing different length scales to facilitate self-assembly.^[99] Figure 2B-c depicts an example of hierarchical structure formation by synthetic polymers through biomimetic folding and self-assembly at multiple scales, modeled via molecular dynamic simulations at different concentrations.^[100] Among copolymer types, block copolymers are among the most extensively studied, typically comprising two (di-) or three (tri-) chemically distinct monomers linked by covalent bonds. These block copolymers can self-assemble into micro- or mesostructures with nanometer-scale features, driven by the volume fraction of each polymer block, as illustrated in Figure 2B-d.^[101] This self-assembly leads to hierarchical organization across different scales due to the interplay of competing interactions between the polymer blocks. Moreover, copolymerization techniques improve polymer performance by enhancing properties like mechanical strength and corrosion resistance, making them suitable for applications such as gas separation membranes. Copolymers can also be synthesized using methods like free radical polymerization, offering cost-effective production and customization.^[102] The versatility of copolymers makes them highly valuable across various industries, including coatings, electronics, and biomedical fields.^[103]

For example, biocompatible copolymers are versatile materials designed for various biomedical applications, particularly in tissue engineering and drug delivery. They are advanced materials designed to interact safely with biological systems, making them essential in various biomedical applications. These polymers can be synthesized to exhibit specific properties such as hydrophilicity, biodegradability, and mechanical strength. For instance, amphiphilic heterograft copolymers have been developed with biocompatible and biodegradable grafts, enabling self-assembly into various morphologies like nanospheres and vesicles, which are crucial for drug encapsulation.^[104] Additionally, dynamic hydrogels made from well-defined synthetic copolymers can mimic extracellular matrix properties, providing strain-stiffening and stress relaxation, essential for tissue engineering.^[105] Furthermore, biocompatible sensors utilizing copolymers have been created for intracellular pH monitoring, showcasing their potential in cellular applications.^[106]

Taking Chitosan, a natural polysaccharide as an example. It is well-known for being nontoxic and biodegradable properties. It can be grafted with thermos-responsive polymers to create materials that respond to temperature changes, enhancing their utility in drug delivery applications.^[107] Chitosan-based copolymers are versatile materials derived from chitosan, a biopolymer obtained from chitin through deacetylation. These copolymers exhibit unique properties that make them suitable for various applications, particularly in the biomedical field. Chitosan-graft-polyacrylic acid (Ch-g-PAA) is a copolymer synthesized by grafting acrylic acid onto chitosan.^[108] It exhibits excellent swelling properties and is used for controlled drug release applications, particularly for anti-inflammatory drugs like diclofenac sodium. Chitosan-graphene oxide composite is another example whose combination enhances mechanical strength, electrical conductiv-

ity, and adsorption properties.^[109] It is explored for applications in biosensing, drug delivery, and water treatment. Besides, the PEG modification in chitosan-PEG copolymers can improve the solubility of chitosan in physiological environments, enhances the biocompatibility of quaternized chitosan.^[110] These materials change their solubility based on temperature, making them suitable for applications that require controlled drug release or injectable hydrogels that gel at body temperature. These polymers can be further categorized into lower critical solution temperature (LCST) and upper critical solution temperature (UCST) types. Poly(*N*-isopropylacrylamide) (PNIPAM), one of the most studied thermos-responsive polymers, is known for its LCST of around 32 °C.^[111] Below this temperature, PNIPAM is hydrophilic and soluble in water, while above it becomes hydrophobic and precipitates out of solution. PNIPAM grafts have been used for applications in intelligent surfaces for cell culture systems as temperature-responsive cell culture surfaces (TRCS) where cell attachment and detachment are modulated by mild temperature changes.^[112]

Similar to biocompatible copolymers, sustainable copolymers are innovative materials designed to address environmental challenges while providing functional properties for diverse applications. Derived from renewable resources, these copolymers offer biodegradability, making them a promising alternative to traditional petroleum-based plastics. Commonly synthesized from bio-based feedstocks like plant sugars or lactic acid, they can naturally decompose, reducing plastic waste. Through copolymerization with various monomers, their properties can be fine-tuned to enhance mechanical strength, thermal stability, and functionalities such as improved adhesion or flexibility. PLA and its copolymers are prime examples of sustainable materials with applications in both biomedical fields and environmental solutions. Derived from agricultural feedstocks like corn and sugarcane, the greenhouse gas (GHG) emission of PLA is 1.3–1.7 kg CO₂e per kg, significantly less than conventional plastics like fossil-derived polyethylene, which emit 2.6–3 kg CO₂e per kg.^[113,114] PLA is biodegradable under industrial composting conditions, achieving 90% decomposition within 180 days, which drastically reduces environmental persistence compared to traditional plastics that can last centuries.^[115,116] In biomedical fields, PLA and its copolymers, such as PLGA, are FDA-approved for applications like drug delivery and tissue engineering due to their biocompatibility and controlled biodegradation, with complete bioabsorption occurring within weeks.^[117] Environmentally, PLA is used in single-use packaging, where it decomposes 20 times faster than polyethylene under landfill conditions,^[118] and its recyclability, with depolymerization efficiencies reaching 90%, supports a circular economy. Poly(butylene succinate) (PBSu) copolymers offer improved thermal transitions and mobility,^[119] boosting performance while retaining biodegradability. Recent efforts have also centered on developing biodegradable conducting polymers that merge electroactivity with sustainability, especially for use in biomedical devices where conductivity and biocompatibility are essential.^[120,121]

3. Multiscale Modeling of Biopolymer

Biopolymers and bioinspired composites exhibit distinct characteristics across different scales, making hierarchical multiscale

methods widely applicable in computational analysis. Each level, from atomic details to macroscopic behavior, can be described separately. Classical hierarchical computational modeling methods are typically divided into particle-based and field-based approaches, which are summarized in Table 3. Particle-based methods represent biopolymers at resolutions ranging from individual atoms, chemical groups, and monomers to regions of polymer melts or solutions, with effective potentials capturing the relevant physicochemical interactions across length and time scales. Field-based methods, on the other hand, describe systems from the perspective of energy functionals, effective potentials, density fields, and collective dynamic variables, providing a materials-scale understanding. This section will explore the theoretical foundations, applications, and validation of particle-based and field-based modeling in biopolymers and bio-inspired composites.

3.1. Theoretical Background

In the context of biopolymers, molecular dynamics (MD) is the largest-scale modeling method capable of capturing detailed atomic-level information about materials.^[122] State-of-the-art MD simulations can now encompass up to a billion atoms, with simulation timescales reaching 100 nanoseconds, leveraging highly optimized calculations of nonbonded interactions and advanced parallelized MD codes.^[123] Within the scope of atomic MD modeling, it is possible to obtain detailed structural and dynamic information on the interactions of atoms, chemical groups, and short polymer chains (oligomers) in melts and solutions. The basic principles of MD simulations lie in the Newton's second law of motion

$$F_i = m_i a_i \quad (1)$$

where F_i is the force acting on particle i , m_i is the mass of particle i , a_i is the acceleration of particle i .

The forces acting on each particle are derived from a potential energy function

$$F_i = -\partial U / \partial r_i \quad (2)$$

where U is the total potential energy of the system, r_i is the position of particle i .

In biopolymers, interactions include both bonded forces (e.g., bond stretching, angle bending, and dihedral torsions) and nonbonded forces (e.g., van der Waals interactions and electrostatic forces). MD simulations track the evolution of these systems by integrating equations of motion over time, typically using algorithms such as the Verlet or velocity-Verlet method. The accuracy of MD simulations depends heavily on the chosen forcefield, such as CHARMM, AMBER, or GROMOS, which is essential for capturing the structural and dynamic properties of biopolymers. MD offers a detailed view of atomic-level processes, including conformational changes, folding mechanisms, and interactions with solvents, providing valuable insights into biopolymer behavior across various environments and timescales, as further explored in Section 3.2.1.

Due to the limitations in length and time scales, MD simulations cannot capture the microphase separation and for-

mation of higher-order structures in biopolymers. To address these phenomena, different levels of coarse-grained (CG) and mesoscale modeling techniques are required.^[124,125] While these methods can model biopolymer assemblies over longer length scales (i.e., up to millimeters) and time scales (i.e., from tens of microseconds to milliseconds, depending on the degree of coarse-graining), they inevitably reduce the chemical specificity of biopolymers to varying extents. For instance, atomic-level structural features, such as local charge correlations and hydrogen bonding, as well as solvent-specific effects arising from these microscopic interactions, are often lost during coarse-graining. Despite this trade-off, CG methods are highly effective in capturing assembly behaviors driven by large-scale structural organization and immiscibility differences, which are less dependent on microscopic details. The fundamental principle of CG modeling is to simplify the representation of biomolecules by grouping multiple atoms (e.g., an entire amino acid residue) into a single coarse-grained particle.^[126] These particles are connected by bonds and angles and may interact through nonbonded forces. Although CG methods sacrifice many detailed interactions, they focus on capturing the general effects or characteristics of various interactions. By reducing the degrees of freedom and smoothing the energy landscape, CG methods lower computational costs and accelerate the dynamics of the system. Consequently, CG approaches are well-suited for capturing nonlocal properties such as hydrophobicity, hydrophilicity, and solvation differences, providing valuable insights into large-scale biopolymer organization. For example, in 1990, Smit et al. introduced the first CG model for simulating amphiphilic systems,^[127] treating water molecules as water-like particles (w) and hydrophobic tails as oil-like particles (o). The interaction between particles was modeled using the Lennard-Jones potential

$$\phi(r) = 4\epsilon \left[\left(\frac{\sigma}{r} \right)^{12} - \left(\frac{\sigma}{r} \right)^6 \right] \quad (3)$$

with o–o and w–w interactions truncated at 2.5σ to represent hydrophobic behavior, and o–w interactions truncated at $2^{1/6}\sigma$ to ensure repulsion. This model successfully simulated amphiphilic self-assembly into micelles, vesicles, and monolayers and was later extended to biopolymer chain models, representing DNA and proteins.^[128] Although these chain models, with hydrophilic and hydrophobic interactions, are widely used to study polymer dynamics and surface interactions, their simplicity limits their ability to predict the complex mechanical behavior of biomolecules with intricate 3D conformations. Current CG research offers a variety of simplified representations and more rigorous parameterization methods, as detailed in Section 3.2.2.

Dissipative particle dynamics (DPD) and Langevin/Brownian dynamics are also particle-based methods that offer distinct advantages for modeling biopolymers, particularly in systems where thermal fluctuations and hydrodynamic interactions are important. DPD is a mesoscale simulation method designed to model complex fluids and soft matter, including biopolymer systems, by introducing dissipative and random forces that mimic the effects of solvent particles.^[129] DPD differs from MD by incorporating a soft repulsive potential, which allows larger time steps and focuses on hydrodynamic behavior over longer length and time scales. This makes DPD suited for studying phenomena

Table 3. Multiscale computational modeling methods of biopolymer and bioinspired design.

Classification	Methods	Description	Basic Theory	Applications in Biopolymer	Limitations
Particle-based methods	Molecular dynamics (MD)	Particle position updates with forces-driven, nonsmooth velocities to simulate molecular interactions over time	$F_i = m_i \cdot d^2r_i/dt^2$ F_i : force acting on particle i m_i : mass and positions of particles i d^2r_i/dt^2 : acceleration of particle i	Mechanical properties; Structural dynamics; Protein aggregation; Biopolymer adsorption; Cellulose; Interface; Energy dissipation...	<ul style="list-style-type: none"> • Limited to simple-shaped particles • Difficult to handle with external forces like gravity, electrostatics, or aerodynamics
Coarse-grained (CG) modeling	Simplifies systems by grouping atoms into larger particles, with positions reflecting averaged interactions at broader scales.	$F_i = -\nabla_i U_{\text{eff}}(r_1, r_2, \dots, r_N)$ U_{eff} : the effective potential r_1, r_2, \dots, r_N : positions of the CG particles	$F_i = m_i \cdot d^2r_i/dt^2 = \sum_{j \neq i} (F_{ij}^C + F_{ij}^D + F_{ij}^R)$ F_{ij}^C : conservative force F_{ij}^D : dissipative force F_{ij}^R : random force, representing stochastic thermal fluctuations	Mechanical properties; Assembly dynamics; Interface; Collagen modeling; Self-assembly; Protein adsorption...	<ul style="list-style-type: none"> • Sacrifices atomic-level detail, limiting accuracy for interactions and complex behaviors like chemical reactions or fine structures
Dissipative particle dynamics (DPD)	Solves stochastic differential equations considering conservative, dissipative, and random forces to simulate fluid-like behavior	$m_i \cdot d^2r_i/dt^2 = F_i - \gamma dr_i/dt + \eta_i(t)$ $\gamma dr_i/dt$: friction or damping term γ : friction coefficient	$m_i \cdot d^2r_i/dt^2 = F_i - \gamma dr_i/dt + \eta_i(t)$ $\eta_i(t)$: random force (stochastic thermal fluctuations)	Self-assembly; Morphological transitions; Copolymer assemblies; Large-scale flow dynamics; Electrostatic interactions; Biopolymer morphogenesis...	<ul style="list-style-type: none"> • Limited by coarse resolutions such as colloids, blood, polymers • Empirical parameter dependencies
Langevin / Brownian dynamics (BD)	Simulate particle motion that includes deterministic forces and random noise to model the effects of friction and thermal fluctuations			Self-assembly; Phase separation; Interface; Biopolymer collapse; Polymerfluid interactions; Cytoskeletal dynamics...	<ul style="list-style-type: none"> • Limited by neglecting inertial effects • Coarse approximations of solvent interactions • Difficulty modeling high-frequency dynamics
Monte Carlo (MC) simulations	Use rand systems		$P_{\text{accept}} = \min \left(1, \frac{\exp(-\beta E_{\text{new}})}{\exp(-\beta E_{\text{old}})} \right)$ P_{accept} : probability of accepting a new state	Phase behavior; Protein interactions; Self-assembly dynamics; Random sampling; Adsorption kinetics; Droplet formation; Slow kinetics...	<ul style="list-style-type: none"> • Limited by slow convergence • Inefficiency in high-dimensional systems • Difficulty handling time-dependent or dynamic processes
Self-consistent field theory	Models polymer systems by solving mean-field equations to minimize free energy	$\omega(r) = \chi r(r) + \lambda$ χ : Flory-Huggins interaction parameter $\rho(r)$: local polymer density at position r λ : Lagrange multiplier enforcing incompressibility	$(-\frac{\hbar^2}{2m} \nabla^2 + V_{\text{eff}}(r))\psi_i(r) = \epsilon_i \psi_i(r)$ $V_{\text{eff}}(r)$: includes external potential, Hartree potential, and exchange-correlation potential	Polymer phase behavior; Mean-field approximation; Block copolymers; Microphase separation; Equilibrium properties; Self-assembly; Morphology prediction...	<ul style="list-style-type: none"> • Limited by mean-field approximations • Difficulty in capturing fluctuations • Reduced accuracy for complex, dense systems
Density functional theory (DFT)	Calculates electronic structure by modeling electron density to determine system properties		$\psi_i(r)$: Kohn-Sham orbital, ϵ_i : orbital energy	Electronic structure; Quantum mechanics; Charge density; Molecular interactions; Chemical bonding; Energy minimization; Self-assembly; Component segregation...	<ul style="list-style-type: none"> • Limited by approximations in exchange-correlation functionals • High computational cost • Difficulty handling excited states

such as biopolymer self-assembly, vesicle formation, and large-scale conformational changes. Langevin dynamics and Brownian dynamics (BD) are mesoscale modeling techniques that extend MD by introducing stochastic and frictional forces, which simulate the effect of a solvent without explicitly modeling solvent particles. Langevin dynamics introduces a frictional term and a random force term in the Newtonian equation of motion, effectively capturing solvent viscosity and thermal fluctuations. This approach is useful for simulating biopolymers in high-friction environments, such as protein folding or DNA dynamics.^[130] Brownian dynamics simplifies further by neglecting inertia, focusing on overdamped systems where thermal motion dominates.^[131] This method is particularly useful for studying the slow dynamics of large biopolymers or polymers in solution. Both DPD and Langevin/Brownian dynamics differ from traditional MD and CG by incorporating stochastic forces to simulate solvent effects more efficiently and at larger scales. They are commonly applied in biopolymer modeling to study processes like polymer chain diffusion, micelle formation, and interactions with biological membranes, as detailed in Sections 3.2.3 and 3.2.4.

In the particle-based methods described above, capturing dynamic evolution tends to incur significant computational costs. However, particle-based stochastic sampling approaches, which do not require solving equations of motion or following time-dependent trajectories, can bypass the large energy barriers that may take longer to overcome in MD or CG simulations. Monte Carlo (MC) simulations serve as a representative method in stochastic sampling approaches.^[132] MC simulations are computational methods that rely on random sampling to explore the statistical properties of a system, particularly its equilibrium configurations. Unlike MD which integrates the equations of motion, MC simulations use probability-based techniques to generate a series of configurations based on a predefined probability distribution. The theoretical foundation of MC lies in statistical mechanics, where the goal is to sample from a Boltzmann distribution,^[133] given by

$$P(x) \propto e^{-\frac{E(x)}{k_B T}} \quad (4)$$

where $P(x)$ is the probability of a system being in a state with configuration x , $E(x)$ is the energy of the configuration, k_B is the Boltzmann constant, and T is the temperature. Metropolis algorithm is the key in MC simulations, which generates a new configuration x' by making a random change to the current configuration x . The acceptance of the new configuration is determined by a probability function

$$P_{\text{accept}} = \min \left(1, \exp \left(-\frac{E(x') - E(x)}{k_B T} \right) \right) \quad (5)$$

The probabilistic acceptance rule in MC simulations ensures that the system primarily samples low-energy, more probable states, while occasionally exploring higher-energy states to avoid being trapped in local minima. Therefore, MC simulations are widely used in fields such as materials science and biophysics to calculate thermodynamic properties, phase transitions, and structural formations, particularly when equilibrium properties are more important than time-dependent trajectories. For example, in protein folding and free energy landscape exploration, MC

methods effectively overcome energy barriers that might otherwise trap systems in local minima. Furthermore, MC simulations are applied to CG models to study large-scale processes like polymer self-assembly and interactions, providing valuable insights into the structural and thermodynamic behavior of biopolymers, as discussed in Section 3.2.5.

Field-based methods represent a distinct class of computational techniques that focus on continuous fields rather than discrete particles. These continuum-level methods treat microscopic details as average or effective overall influences, allowing for the capture of large-scale material responses. Two prominent field-based methods are self-consistent field theory (SCFT)^[134] and density functional theory (DFT).^[135] SCFT is commonly applied in biopolymer modeling, which predicts the equilibrium structure and phase behavior of complex systems by solving for the spatial distribution of polymer chains in terms of concentration fields. By modeling polymers as continuous fields rather than individual chains, SCFT efficiently captures large-scale phenomena such as phase separation, self-assembly, and polymer blending in biopolymer systems. In contrast, DFT is a quantum mechanical method used to model the electronic structure of molecules and materials, particularly useful for studying smaller biomolecules like nucleic acids, amino acids, or peptide chains. Instead of simulating atomic motions like particle-based methods (e.g., MD or CG), DFT focuses on electron density distribution, providing highly accurate insights into bonding and electronic behavior. This makes it ideal for capturing the quantum mechanical effects in biopolymer interactions, such as hydrogen bonding and charge transfer, which are critical for understanding the chemical specificity of biomolecules. Through continuous fields, field-based methods offer more efficient ways to study long-range interactions and large-scale structures in biopolymers, such as phase behavior in SCFT or quantum-level interactions in DFT, as discussed in Section 3.3.

3.2. Particle-Based Modeling

3.2.1. Molecular Dynamics Modeling

The development of forcefields and accuracy assessment of atomic structures are critical components of atomistic modeling for biopolymers. In MD simulations, the forcefield expresses the potential energy function governing atomic interactions. Accurate forcefields are essential for correctly calculating the potential energy surface, which dictates particle motion and enables precise predictions of key system properties, including structural stability, thermodynamic behavior, and molecular dynamics.^[136] Recent advancements, such as improved parallelization, have enabled simulations to reach microsecond (μs) to millisecond (ms) timescales, allowing more detailed studies of native protein structures, transient states, and assembly processes. Traditional force fields often lacked polarizability, which limited their accuracy in capturing electronic effects, but newer polarizable forcefields now better represent phenomena like protein secondary structure stabilization. Constant-pH MD methods are a key recent innovation, enabling the modeling of protonation state changes in response to pH fluctuations, a crucial factor for biopolymers such as proteins and nucleic acids. These methods improve

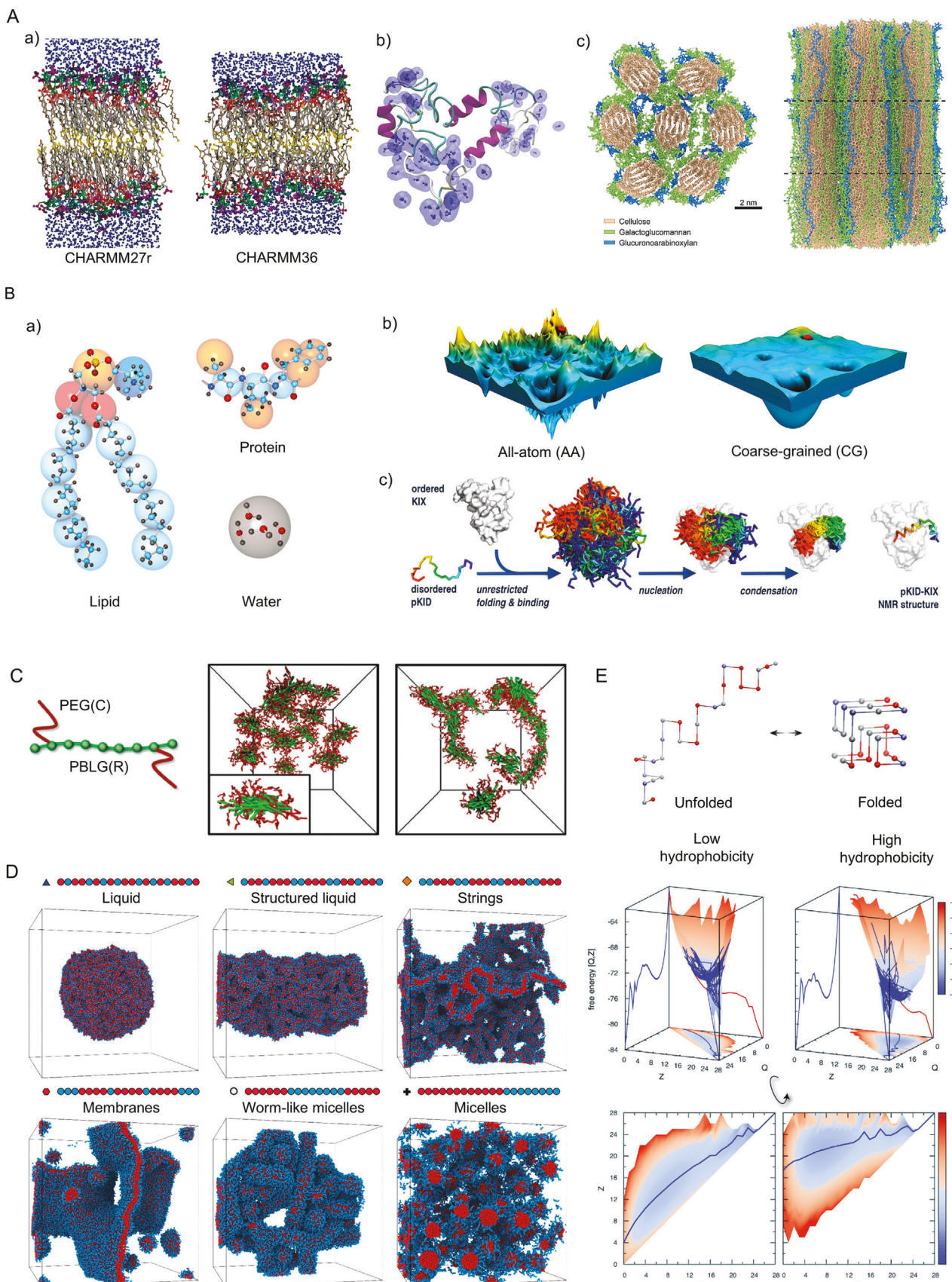
accuracy in simulations where local pKa shifts, influenced by neighboring groups, are critical. Despite these advancements, forcefields like CHARMM and AMBER still exhibit limitations, particularly in modeling intrinsically disordered proteins and nucleic acids, often leading to overly compact conformations due to parameterization based on folded structures. To address these challenges, newer forcefields have been fine-tuned to better balance nonbonded interactions such as salt bridges and hydrophobic effects, improving predictions of protein and nucleic acid structures (Figure 3A-a).^[137] Comparing forcefield predictions with experimental data has become an essential approach for validating models, particularly for systems like poly L-lysine, poly L-glutamic acid, and DNA. The choice of forcefield and parameterization critically influences simulation outcomes, highlighting the importance of selecting models based on their original reference systems and performing experimental verification whenever possible.

The application of full atomistic MD simulations focuses primarily on structural, dynamic, and functional aspects, with a heavier emphasis on biological systems than materials, except in the area of cellulose.^[138–140] For protein-based materials, hierarchical structures play a significant role in their assembly and mechanical properties.^[141,142] Through all-atom MD, it has been revealed that silk-like proteins exhibit nonlinear stress responses that localize deformation, contributing to the mechanical robustness of spider webs.^[143] MD simulations have also explored the role of multiple attractive regions in silk proteins, which form bi-continuous network structures that potentially influence the formation of fiber.^[144] In another study on spidroins (i.e., the primary proteins in spider silk), MD was used to investigate the effects of ethanol as a solvent additive on protein aggregation, solvation environment, and secondary structure (Figure 3A-b).^[145] The results demonstrated that ethanol weakens hydrophobic interactions, providing a tunable assembly mechanism for protein-based materials. Beyond silk, other protein materials, such as elastin-like peptides,^[146–148] collagen fibers,^[58,149,150] and polypeptides,^[151,152] have been investigated using MD and CG simulations to study mechanical properties, critical solution temperature responses, and energy dissipation in protein-based materials. Additionally, MD has been employed to explore biopolymer adsorption, particularly the interaction between peptides and surfaces such as silica nanoparticles, mapping how pH, particle size, and charge influence adsorption. Despite these insights, the limitations of MD regarding length and time scales pose challenges in studying phenomena like film formation and collective adsorption effects. Regarding cellulose-based composites, MD simulations focus on interactions between cellulose nanofibrils (CNFs), hemicellulose, and lignin, essential for understanding the mechanical properties of materials like wood (Figure 3A-c).^[153] Simulations have shown that hemicellulose lies flat on cellulose surfaces.^[154,155] Meanwhile, lignin occupies the matrix, which contributes to material distribution within the wood cell wall. Mechanical loading studies reveal elastic and yield behavior driven by matrix molecule reorganization and CNF sliding, breaking and reconstructing hydrogen bonds.^[156–158] However, while these models provide molecular-level insights, they lack mesoscale structural features such as microfibril angles, limiting their ability to capture comprehensive wood mechanics.

3.2.2. Coarse-Grained Modeling

CG models simplify atomistic or molecular details of biopolymers by grouping atoms into CG beads, balancing detail with the ability to simulate larger systems and longer time scales. Two primary approaches exist for defining effective CG interactions: bottom-up structure-based coarse-graining, which derives potential from atomistic MD simulations, and top-down thermodynamics-based coarse-graining, which fits interactions to experimental data.^[126,159,160] While the former preserves chemical specificity, the latter produces more transferable potentials.^[126,161] Many CG models use a combination of both approaches to iteratively refine forcefield parameters. A notable example is the MARTINI forcefield, which represents groups of atoms with specific CG bead types and models nonbonded interactions using a Lennard-Jones potential fitted to thermodynamic data like partition-free energies, while bonded interactions are tuned to atomistic MD distributions. MARTINI has been expanded to simulate proteins, DNA, RNA, polysaccharides, and synthetic polymers, though it was originally designed for lipids (Figure 3B-a).^[162] However, its implicit solvent variant, Dry MARTINI, speeds up simulations but is limited by its inability to model soluble proteins or equilibrium between membrane-bound and dissolved compounds. Another widely used CG forcefield, SIRAH, avoids MARTINI's constraints on protein secondary structure and allows for protein-DNA complex modeling. Similarly, models like UNRES, SURPASS, and PRIMO extend CG capabilities to various biomolecules, including membrane proteins, by providing a smooth energy landscape compared with all-atom (AA) model (Figure 3B-b).^[162] One challenge with CG models is that coarse-graining reduces the system's entropy due to fewer degrees of freedom, which is often compensated by increasing enthalpic contributions, particularly in implicit solvent models like Dry MARTINI.^[163] Recent advancements also focus on improving CG models by reparametrizing forcefields to better capture hydrogen bonding and electronic polarizability, as seen in the updated MARTINI forcefield.^[164] Additionally, ML is emerging as a tool for generating CG forcefields by deriving interaction potential from quantum mechanical calculations, providing new avenues for CG model development.

The application of CG modeling in biopolymer systems allows for the investigation of complex behaviors at larger time and length scales. Examples include the exploration of the mechanical properties of collagen,^[165] oligonucleic acid backbone chemistry variations on hybridization and melting thermodynamics,^[166] as well as the thermodynamics and assembly of multiarm oligonucleic acid star polymer conjugates.^[167] CG modeling has also been used to investigate interactions at interfaces, including protein folding and binding (Figure 3B-c),^[168] substrate patterning, and film morphology in lamellar phase copolymers under different thermal and substrate conditions.^[124,169] A combination of all-atom and CG modeling has proven valuable for studying intrinsically disordered proteins at interfaces, elastin-like peptides' lower critical solution temperature, and collagen-mimetic fibril formation.^[147,148,170] Additionally, the self-assembly of tropoelastin into fibrils has been explored using the CG MARTINI forcefield.^[170] Polyethylene glycol (PEG) polymers and PEG-conjugated lipids have also been modeled in bulk and at interfaces with proteins or surfaces,



highlighting their importance in bioengineering and drug delivery applications.^[171,172] A minimal CG model has recently been developed to account for the heterogeneity of intrinsically disordered proteins in nuclear pore complexes, validated against experimental data on single-molecule interactions with nuclear transport receptors.^[173] Reviews have also highlighted the application of CG models to colloid and protein adsorption.^[174] In cellulose modeling, CG methods have been used to match the mechanical responses of atomistic models, extending the scale to hundreds of nanometers to assess the mechanical properties of wood cell walls with various microfibril angles. As the microfibril angle increases, cellulose nanofibrils deviate from the primary load-bearing direction, softening the material, with matrix molecule sliding becoming more prominent.^[175,176] These examples illustrate the versatility of CG models in capturing biopolymer behavior, enabling detailed studies of assembly, mechanical properties, and interface interactions across multiple scales.

3.2.3. Dissipative Particle Dynamics

DPD is a coarse-grained, particle-based simulation model using soft-core potentials, designed to capture the hydrodynamic behavior and time evolution of fluid-like systems.^[129] DPD operates effectively at mesoscopic scales, capturing structural and morphological changes, as well as large-scale flow dynamics, which are particularly relevant in biopolymer modeling. Unlike CG modeling, DPD can simulate self-assembly and morphological transitions that occur over extended time scales. This is particularly valuable for studying copolymer assemblies, which exhibit diverse morphologies in response to environmental stimuli, such as spheres, vesicles, and lamellar phases.^[177] A notable example includes the self-assembly of bio-based block copolymers like poly 1,2-butadiene-b-polyethylene oxide (PB-b-PEO) in ionic liquids, where DPD simulations revealed a wide range of assembled structures dependent on polymer concentration and block length ratios.^[178] Biopolymer systems with hierarchical structures are well-suited for DPD, provided the assembly behavior is governed by effective bead-bead interactions rather than highly localized forces.^[179] For instance, DPD has been used to model the higher-order self-assembly of copolymer micelles into complex structures like nanowires, as seen with PBLG-g-PEG micelles (Figure 3C).^[180] DPD simulations also extend to silk protein fiber assembly, where the protein is treated as a multi-block copolymer to explore processing conditions and design parameters.^[179] The high level of coarse-graining achievable with

DPD allows it to capture large-scale self-assembly phenomena, such as protein aggregation and polymer self-assembly in 2D environments. For example, DPD simulations have demonstrated entropy-induced attractions between protein complexes in lipid bilayers, driven by complementary shapes.^[181] The method has also been applied to study polymer self-assembly in solution, revealing structures such as rods, bent rods, and rings based on the mix ratio of linear and branched polymers. Confinement effects in self-assembly have also been investigated, showing that constrained geometries (e.g., vesicle curvature) can lead to unique structures not observed in bulk (e.g., U-shaped and ring-like vesicles). Furthermore, DPD has been expanded to include electrostatic interactions and polarizability.^[182–184] Although polarizability reduces the achievable level of CG, it enables accurate modeling of protein folding and native structures. These advancements make DPD an essential tool for studying large-scale biopolymer self-assembly, morphogenesis, and interaction with complex environments.^[119]

3.2.4. Langevin/Brownian Dynamics

Langevin dynamics^[125] and BD^[185] are both stochastic simulation methods for modeling systems with thermal fluctuations, particularly in biopolymer modeling. Langevin dynamics extends classical MD by adding a frictional force and a random noise term to Newton's equation of motion, effectively simulating the interaction of particles with an implicit solvent. This approach is ideal for studying systems where solvent viscosity and temperature effects are important, such as protein folding or diffusion in viscous environments.^[130] In contrast, BD simplifies the system by neglecting inertia, meaning the acceleration term is omitted. This makes BD suitable for systems dominated by thermal motion, such as large macromolecules in solution, where frictional forces are much stronger than inertia.^[186] Both BD and Langevin dynamics use stochastic methods to account for thermal fluctuations. However, Langevin dynamics retains inertia, making it better for systems with moderate to high friction. BD is ideal for slow dynamics in overdamped systems. While Langevin dynamics can model a wider range of timescales and behaviors, BD is more computationally efficient when inertia is negligible. Both methods are widely used to study diffusion, conformational changes, and the self-assembly of biopolymers.

Langevin dynamics is a powerful CG method for large-scale simulations of biopolymers, effectively bridging time and length

Figure 3. Particle-based methods for the computational modeling of biopolymers. A) Molecular dynamics (MD) modeling: a) critical improvement to simulations of lipid–protein bilayers resulting from changes to CHARMM36 to CHARMM27r forcefield. In CHARMM27r, the bilayer phase transitioned inappropriately to gel phase, while CHARMM36 maintains liquid-crystalline phase; Adapted with permission.^[137] Copyright 2011, American Chemical Society. b) distribution of the solvent around the protein molecule: water molecules in the 94% ethanol concentration solvent system; Adapted with permission.^[145] Copyright 2023, American Chemical Society. c) cellulose microfibril bundle along the fibril axis and perpendicular to the fibril axis; Adapted with permission.^[153] Copyright 2021, Elsevier. B) Coarse-grained (CG) modeling: a) all-atom versus CG representation in the MARTINI model; Adapted with permission.^[162] Copyright 2016, American Chemical Society. b) schematic illustration of the rugged and complex energy landscape of an AA model compared to the smooth surface in a CG model; Adapted with permission.^[162] Copyright 2016, American Chemical Society. c) mechanism of coupled folding and binding of the pKID/KIX complex; Adapted with permission.^[168] Copyright 2014, American Chemical Society. C) Dissipative particle dynamics (DPD) model of a rod-g-coil graft copolymer with simulation snapshots of spindle-like subunits and nanowire aggregates; Adapted with permission.^[180] Copyright 2016, Wiley. D) Langevin/Brownian dynamics (BD) for CG modeling of intrinsically disordered proteins at fixed degree of hydrophobicity (red beads) and temperature; Adapted with permission.^[189] Copyright 2020, AIP Publishing. E. Monte Carlo (MC) simulations of protein-like lattice model folding in the free-energy landscape. Adapted with permission.^[203] Copyright 2018, AIP Publishing.

scales while addressing both assembly and dynamics. Despite the challenges of constructing accurate interaction models and parameter matching, it is highly effective for modeling biopolymer behavior. For example, CG Langevin dynamics has been used to explore how polymer conjugation affects the hybridization thermodynamics of oligonucleic acids and how macromolecular crowding influences biopolymer collapse.^[187,188] By incorporating scaling arguments and low-friction dynamics, these models can accurately predict polymer size based on volume fraction. Langevin dynamics is also applied to protein diffusion in lipid bilayers and has become useful in studying intrinsically disordered proteins (IDPs). These models account for steric, hydrophobic, and electrostatic interactions between residues (Figure 3D).^[189] In the study of liquid-liquid phase separation, CG Langevin simulations have revealed complex phase behaviors, such as the formation of liquid, membrane-like, and micellar structures, driven by subtle changes in hydrophobic and hydrophilic sequence patterns.^[190] Additionally, Langevin dynamics has been used to investigate active polymers adsorbed on cylindrical surfaces, providing insights into polymer-fluid interactions and electrophoretic transport through synthetic nanopores. In biopolymer networks with active motors, simulations have shown strain stiffening under increased shear deformation, a key characteristic of cytoskeletal networks.^[191] This method is particularly valuable in modeling the dynamics of actin-based cytoskeletal networks, offering insights into mechanisms critical to cellular processes.^[192] Furthermore, Langevin dynamics can simulate single protein conformations at constant pH,^[193] making it a versatile tool for studying complex biological systems, sensor applications, and molecular switches.

BD is widely used to model biopolymer systems, particularly in crowded environments such as cells.^[194] BD has been applied to study proteins, with a recent focus on liquid-liquid phase separation. For example, a CG bead-spring model combined with BD has shown how silk-like block proteins' length and concentration affect self-assembly morphologies.^[195] BD simulations have also examined the role of charge in RNA and modular proteins, revealing that nonspecific interactions significantly influence droplet formation in phase separation at low protein-polymer interaction energies. In protein solutions, BD retains atomistic detail while treating the solvent as a continuous medium, resulting in quantitative agreement with experimental data.^[196] BD methods are also used to model polymeric networks, where crosslink density and topology affect their mechanical properties.^[197,198] In protein hydrogels, the initial volume fraction is the key to network assembly, but single protein characteristics also play a role. A hybrid BD approach has integrated mean field models of hydrodynamic interactions with automatically detailed protein simulations, revealing the importance of weak protein-protein and solvent-mediated interactions in concentrated protein solutions.^[199] BD has also been employed to model the self-assembly of amyloid-forming proteins and to study the ejection dynamics of active polymers through small pores, identifying entropy-driven, force-accelerated, and force-dominated stages in the process.^[200] Finally, BD techniques have been generalized to model diffusive phenomena in biological systems, making them broadly applicable for studying the dynamic behavior of biopolymers in various environments.^[201]

3.2.5. Monte Carlo Simulations

Particle-based approaches like MD use deterministic numerical integration to track system evolution, while methods like DPD, Langevin, and Brownian dynamics include stochastic noise and dissipative forces. In contrast, MC simulations rely on stochastic sampling of possible system states rather than time-dependent integration. The most common approach, the Metropolis MC method, samples system states with weights corresponding to the Boltzmann distribution, typically within the NVT ensemble.^[132] While this method focuses on equilibrium properties, more advanced MC variants (e.g., NpT and Grand Canonical MC) allow sampling other ensembles, with applications including ligand-protein binding. Although MC methods generally lack kinetic information, kinetic MC algorithms exist to address this limitation.^[202] MC simulations are often implemented on a lattice, especially in biopolymer modeling, due to their efficiency in sampling complex systems (Figure 3E).^[203] Recent MC studies have applied CG approaches to biopolymers, such as protein amyloids.^[204] These studies explored amyloid fibril formation, oligomer dynamics, and protein aggregation on cell membranes, revealing key pathways in macromolecular aggregation and the influence of lipid membrane properties, such as fluidity and protein-membrane affinity, on protein aggregate morphology and nucleation pathways.^[205–207]

MC methods have also been extensively used to study liquid-liquid phase separation and protein systems with anisotropic, patchy interactions.^[208,209] Hybrid approaches that integrate molecular-level MC simulations into single chain in mean-field simulations have successfully linked molecular structure to large-scale polymer self-assembly.^[210] MC modeling has been employed to investigate phase behavior in *Caenorhabditis elegans* protein LAF-1 droplets, combining fluorescence correlation spectroscopy with theoretical insights from AA MC simulations.^[211] These studies have elucidated the interactions driving phase separation and droplet formation. Additionally, the kinetics of poly-L-lysine adsorption on silica surfaces have been explored using MC simulations combined with experiments, following the random sequential adsorption scheme.^[212] MC approaches have also proven particularly powerful for predicting biopolymer structures, uncovering key molecular interactions and dynamic processes that govern self-assembly, phase behavior, and adsorption in biological and synthetic systems.^[213–215]

3.3. Field-Based Modeling

3.3.1. Self-Consistent Field Theory

SCFT, a CG mean-field approach, has proven highly effective for modeling biopolymers by simplifying complex molecular interactions through the assumption of Gaussian-distributed monomers along polymer chains.^[134] Initially developed for polymer systems such as polymer brushes, homopolymer interfaces, and block copolymer microstructures,^[134] SCFT has since been extended to more intricate macromolecular structures, including dendrimers,^[216] ring polymers,^[216] and star copolymers,^[158] as well as processes like liquid-liquid phase separation in amphiphilic systems.^[217,218] The core strength of SCFT lies in its

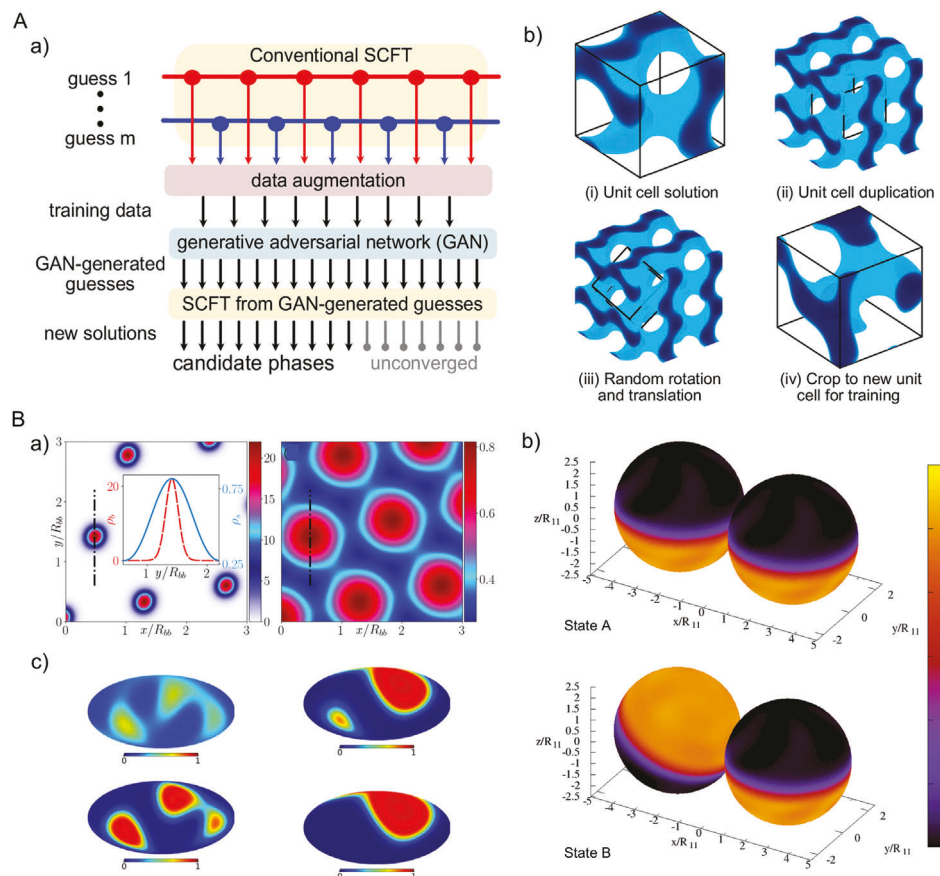


Figure 4. Field-based methods for the computational modeling of biopolymers. A) Self-consistent field theory (SCFT): generative polymer field theory for block polymer phase discovery a) the pipeline illustration of this generative approach; b) example of a data augmentation strategy involves duplicating the unit cell during an SCFT trajectory, followed by random translation, rotation, and extracting a new unit cell for training data; Adapted with permission.^[220] Copyright 2023, National Academics Press. B) Density functional theory (DFT) a) single length scale self-assembled phase, refers to micelles in polymer systems or droplets forming in a regular emulsion; Adapted with permission.^[222] Copyright 2021, American Physical Society. b) phase separation dynamics on spherical surfaces through minimal DFT. The plot shows two different configurations "A" and "B". State "A" is the configuration with a minimal energy cost. Turning one of the spheres away from this configuration (state "B") leads to an extra energy cost; Adapted with permission.^[227] Copyright 2016, American Physical Society. c) Mollweide projection of equal area pixelization for the dynamic DFT calculation data showing evolution of the particle density for the small sphere. Adapted with permission.^[228] Copyright 2019, IOP Publishing.

ability to capture the spatial distributions of molecular components, making it especially useful for predicting large-scale assembly and phase behavior in biopolymer systems. Relevant to both biological systems and industrial applications, SCFT has been used to model polysaccharide-protein mixtures which offer insights into their thermodynamic stability and structural organization.^[219] Recently, SCFT has also been used as a screening tool to guide experimental design. To address the challenge of discovering new morphologies, a deep convolutional GAN is trained on SCFT solutions. This approach has generated hundreds of candidate polymer phases, including previously unexplored structures, by leveraging the trajectories from converged SCFT simulations (Figure 4A).^[220]

3.3.2. Density Functional Theory

DFT is an effective approach for studying structure formation, assembly, and dynamic reorganization in polymeric systems. DFT

is particularly useful for modeling pattern formation, component segregation, and phase separation on mesoscopic and continuum length scales. Classical DFT (cDFT) operates by expressing the thermodynamic potential (e.g., free energy in the NVT ensemble or grand canonical potential in the μ VT ensemble) as a density-dependent functional, which is minimized to resolve the system's density distribution. While cDFT sacrifices chemical specificity due to the effective nature of its interaction models, it excels at providing insights into large-scale phenomena like phase separation, self-assembly, and transport, which are otherwise inaccessible to more detailed approaches. For example, DFT has identified key intermolecular interactions responsible for complex self-assembled structures in binary polymer mixtures,^[221] offering guidance for controlling material assembly in polymeric and protein-based systems. DFT has also been combined with DPD to investigate the emergence of structures with competing length scales in soft matter,^[222] providing insight into the phase behavior and crystallization in dendrimers and star polymers (Figure 4B-a). These studies revealed rich

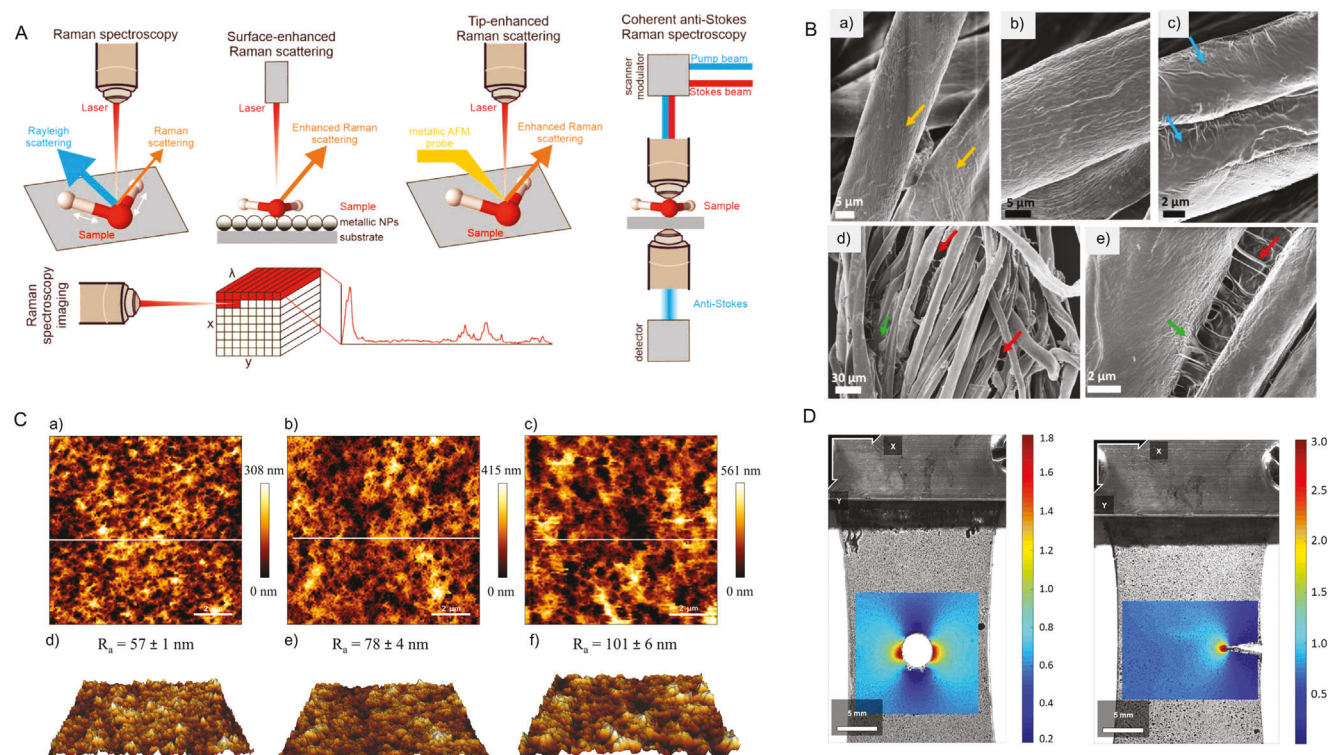


Figure 5. Experimental approaches for the characterization of biopolymers. A) Raman spectroscopy, surface-enhanced Raman scattering, tip-enhanced Raman scattering, coherent anti-Stokes Raman spectroscopy, and Raman spectroscopic imaging; Adapted with permission. [230] Copyright 2023, MDPI. B) SEM images of cotton fibers treated with a) water, b,c) ethanaminium 2-hydroxyN,N-bis(2-hydroxyethyl)-N-methyl-esters (TEQ) 1 wt%, d,e) TEQ 1 wt% in presence of guar biopolymers; Adapted with permission. [233] Copyright 2021, MDPI. C) AFM height images with varying concentrations of alginate and calcium. a,d) 2.0% (w/v) alginate and 22×10^{-3} M CaCO_3 , b,e) 1.0% (w/v) alginate and 18×10^{-3} M CaCO_3 , and c,f) 0.5% (w/v) alginate and 15×10^{-3} M CaCO_3 . R_a is given as $\text{SEM} \pm \text{STDEV}$ for $n = 3$ gel surfaces. Scale bar is $2 \mu\text{m}$; Adapted with permission. [234] Copyright 2022, Elsevier. D) Longitudinal strain distribution of poly(vinyl alcohol) (PVA) hydrogel crosslinked by transient (physical) and covalent (chemical) bonds in circular hole and semicircular edge notch using DIC method. Adapted with permission. [236] Copyright 2019, Springer Nature.

phase behaviors, including two crystalline phases, a fluid phase, and metastable quasicrystal structures, particularly in systems where monomers exhibit contrasting hydrophilic and hydrophobic properties across generations. [223,224] Moreover, DFT has been employed to explore the adsorption kinetics of globular proteins onto charged core-shell microgel particles, validated against experimental data for lysozyme adsorption on PNIPAM-coated nanoparticles. [225] DFT's predictive capability extends to the self-assembly of sphere-forming di-block copolymers in confined environments, such as square wells and cylindrical nanopores, where it accurately maps morphological transitions. [226] In another example, a minimal DFT model was used to study phase separation dynamics on spherical surfaces, motivated by heterogeneous domain structures observed on cell membranes (Figure 4B-b). [227] This study found that the size of the sphere influenced the dynamical response, with further analysis using power spectra and Minkowski functionals confirming the size-dependent phase behavior (Figure 4B-c). [228]

3.4. Experimental Validation

Besides various computational modeling approaches to understand biopolymers better, various experimental methods are also

involved to measure and quantify the properties of biopolymers in different scales.

In nano and mesoscale, Raman spectroscopy is often used to identify the chemicals using the spectral fingerprint, quantify the concentration or amount of chemicals, and reveal crystallographic orientation and crystallinity of polymers through interpretation of the Raman spectrum. The Raman spectrum is usually obtained by shining a laser onto the sample based on the Raman effect. [229] With the advances in lasers, detectors and computing power, Raman spectroscopy has become an important tool in materials characterization (Figure 5A). [230] To get a better visual inspection of the sample, especially the surface feature, scanning electron microscope (SEM) [231] and atomic force microscope (AFM) [232] are two commonly used devices. The former one utilizes a focused beam of high-energy electrons to reveal the detailed surface characteristics through analyzing the signals after the electrons interact with the atoms in the sample (Figure 5B). [233] The latter one creates images by moving a small cantilever across the surface of a sample. When the tip at the end of the cantilever touches the surface, it causes the cantilever to bend, which changes the amount of laser light reflected into the photodiode. The height of the cantilever is adjusted accordingly to restore the response signal and hence trace the surface (Figure 5C). [234] Both

methods provide high-resolution imaging and analysis of surfaces in detail.

Under micro- and macro-scale range, emphasis has been placed on the evaluation of porosity, cracks, and damages. For instance, X-ray inspection methods are used to examine the internal structure of objects without damaging them. It works by directing X-rays onto the sample and the radiation that passes through is captured on the detector, creating an image based on the varying absorption of the material. Moreover, a 3D profile can be reconstructed by stacking multiple 2D images from different depths or angles, commonly referred as computed tomography (CT). Besides, in order to capture the dynamic changes of a sample under measurement, digital image correlation (DIC) provides an optical-based approach to measure full-field strains of the specimen.^[235] It works by capturing images of the sample before, during, and after the deformation, along with tracking the movement of specific patterns or features on the surface to calculate how much the material has deformed (Figure 5D).^[236] DIC offers a noncontact visualization technique to evaluate the samples under complex dynamic testings such as vibrations, impact, or high-speed deformations.

In addition to experimental approaches and devices that are used to characterize the materials, the fabrication of biopolymers is another critical aspect to prototype the desired structures. Due to the increased complexity of biopolymers including composite materials, intricate designs, and fabrication procedures, additive manufacturing methods have shown promising achievements in creating multimaterial, multiscale, and multi-functional prototypes that are difficult to fabricate using conventional approaches.^[237,238] A wide range of biopolymers including polysaccharide (i.e., starch, alginate, and chitosan) and protein (i.e., silk, collagen, and gelatin) are printed using direct ink writing, binder jetting, or stereolithography techniques.^[239] The capability of physically prototyping the virtual modeling biopolymers is an indispensable counterpart to fulfill the final objectives and functionalities.

4. AI-Enabled, Advanced Biopolymer and Bioinspired Designs

The multiscale architecture of biopolymers and bio-inspired composites provides special functionality of the material with unique properties. Various modeling approaches are conducted to explore the mechanism on different scales. Due to the increased computational complexity and cost, it has been a long-lasting challenge to comprehensively understand the processing-structure-property relationships and generate superior designs. In this section, solutions given from ML are discussed in biopolymer characterization, fabrication process, and design prototyping aspects.

4.1. Biopolymer Characterization

With the establishment of multiple polymer databases such as in-house prepared datasets, PoLyInfo, and PI1M that contain over ten thousand polymers for polymer informatics with about a hundred critical properties, researchers are able to build analytical

models to understand the relationships between properties and structures for biopolymers.^[240] For instance, a multitask deep neural network property predictor was developed for polyhydroxylalkanoates (PHAs), a type of bio-synthesized and biodegradable bioplastics.^[241] Based on the open-source experimental data that include nearly 23 000 homo- and copolymer chemistries, the predictor was able to identify 13 key thermal, mechanical, and gas permeability properties with outstanding overall coefficient of determination (R^2) values (Figure 6A). Additionally, the predictive model was subsequently utilized to find bioreplacements for seven commodity plastics, leading to two bioreplacements for each commodity plastic that have superior properties with possible chemical synthesis and biosynthesis routes. For specific applications without existing open-source datasets, data-driven approaches have been utilized to realize comprehensive characterization of desired properties in a large design space. In a recent study, high-throughput MD simulations were performed to build ML models that predict the glass transition temperature of biopolymers (Figure 6B).^[242] A dataset comprising 546 polymers was generated, which includes 58 homopolymers and 488 copolymers through 2184 MD simulations. Based on the simulation data points, multiple ML algorithms including logistic regression, k-nearest neighbors, support vector machines, and ensemble learning algorithms were performed to achieve a mean absolute error of 19.34 K and an R^2 score of 0.83 when predicting the MD-calculated glass transition temperatures. In addition, to establish the analytical relationship between property and polymer structure, a notation standard, SMILES (Simplified Molecular Input Line Entry System) that represents the structure of chemical species in the form of a line notation using short ASCII strings (letters and symbols) was used. This standard naming convention provides direct opportunities for ML tasks such as feature embedding, baseline comparison, and adaptivity to utilizing language models. Conventionally, the symbol representation of the polymer structure can be further encoded into numbers through molecular descriptors calculated from the polymer repeat units with open-access packages such as Mordred.^[243] However, with the advancement of large language models, new approaches have been explored to better encode the symbolic polymer structures. For example, transformer-based language models such as TransPolymer,^[244] and polyBERT^[245] were developed for polymer property prediction. Transformer architecture shows superior capability to capture long-range dependencies in structure strings using attention mechanisms. Moreover, the trained encoder architecture such as the polyBERT model can be fine-tuned for other downstream tasks, providing enhanced transferability.

4.2. Fabrication Process Optimization

Besides leveraging AI approaches in the computational domain for biopolymer characterization, AI-driven methods were also actively applied in the fabrication process to determine better process parameters.^[34,246] To realize the different functionalities of various biopolymers with distinct structures and compositions, a series of processing and fabrication methods were developed including solvent casting, electrospinning, injection molding, and heat pressing.^[247,248] For instance, alginate films were

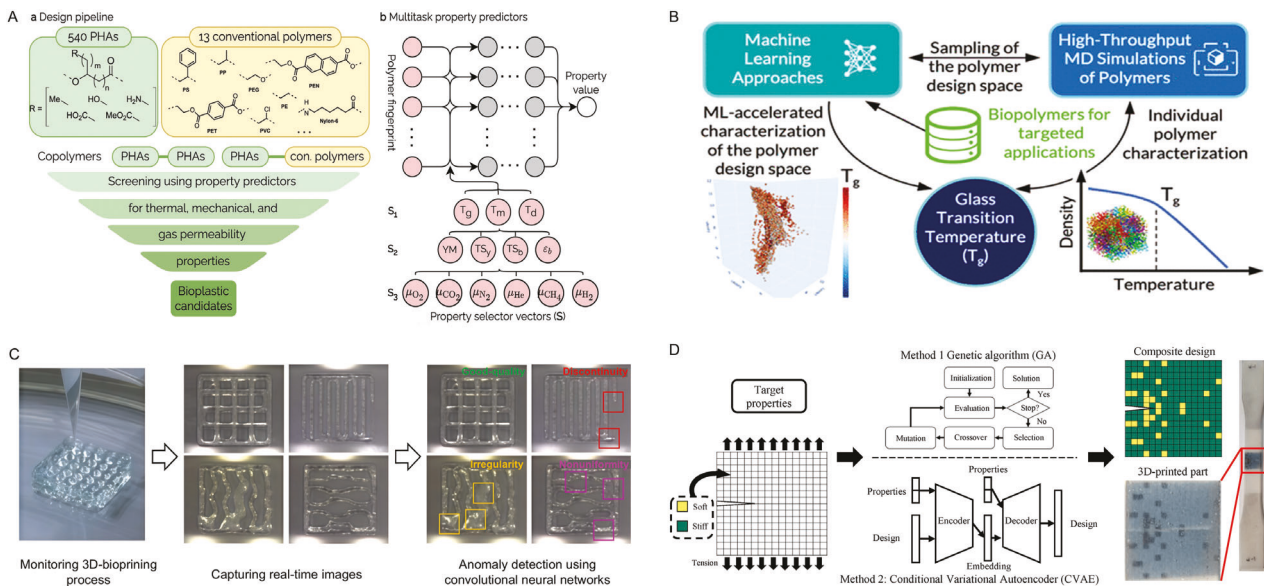


Figure 6. AI-enabled, advanced biopolymer and bio-inspired designs. A) The design pipeline of combining 540 polyhydroxyalcanoates (PHAs) with 13 conventional polymers to copolymers and the architecture of the multitask neural network predictors; Adapted with permission.^[241] Copyright 2022, Springer Nature. B) Illustration of using high-throughput molecular dynamics simulations and machine learning to predict the glass transition temperature of biopolymers; Adapted with permission.^[242] Copyright 2024, American Chemical Society. C) Convolutional neural networks based real-time anomaly detection for 3D-bioprinting processes; Adapted with permission.^[252] Copyright 2023, American Chemical Society. D) Flowchart of using genetic algorithms and conditional variational autoencoders to design bioinspired composite structures. Adapted with permission.^[264] Copyright 2023, MDPI.

prepared by solvent casting technique for antibacterial wound dressing applications;^[249] chitosan membranes were fabricated using post-electrospinning treatment for guided bone regeneration;^[250] and biodegradable thermoplastic cassava starch/sodium alginate composites^[251] were created using injection molding for enhanced mechanical properties. Besides these processing techniques, 3D-bioprinting methods provide a unique way to realize customizable prototypes that are difficult to fabricate using conventional methods. With the advancement of AI algorithms, promising results have been presented to realize prints with high printing quality and advanced properties under optimal processing conditions. For instance, Jin et al., utilized camera devices and CNN algorithms to realize layer-wise defects detection during the 3D bioprinting process of GelMA material (Figure 6C).^[252] Even for transparent GelMA material, the model was able to reach satisfactory performance in classifying different defects that happened during the printing process. Bone et al., built a hierarchical ML model based on deep neural networks to predict and optimize the print fidelity of alginate hydrogel 3D prints through refining printing parameters including flow rate, printhead traveling velocity, and nozzle diameter.^[253] Besides reaching better fabrication quality, the mechanical properties of the prints can be improved as well. For example, the ultimate tensile strength of 3D-printed polyether ether ketone (PEEK) specimen was optimized by modifying infill density, infill patterns, as well as layer height, and printing speed during fabrication.^[254] By building an ML regression model using support vector machine and random forest models based on the experimental data, optimized candidate process parameters were proposed using genetic algorithms. Considering the high cost and increasing efforts for physical

experiments, other AI algorithms were actively utilized to reduce the amount of data collection and manual operating procedures. For example, Yang et al. used small amount of experimental data and neural network models to predict the optimal processing condition that leads to the highest specific mechanical properties for mycelium-based wood composites.^[248] The machine learning method demonstrated the ability to predict outcomes in a high-dimensional design space that experiments cannot comprehensively explore. The ML predictive model could also reveal complex relationships between input factors such as process and design parameters against output objectives such as fabrication quality and material properties. Bayesian optimization (BO) methods are able to perform process optimization tasks based on a small amount of experimental data through Gaussian process surrogate modeling and probabilistic estimation. In this study, the printability and resolution of PCL-MgO nanocomposite were optimized by only 11 iterations of refining printing speed, pressure, and nozzle temperature.^[255] Moreover, such processes can be fully augmented in automation and real-time monitoring using cameras and programmed robotic arms in autonomous labs. For instance, A-Lab, a fully automated materials-discovery laboratory, realized synthesizing novel compounds with a high success rate (71%) and faster speed than human operator.^[256] This platform provided an interdisciplinary thrust that combines robotic automation and data-driven ML methods to experimentally validate predictions made on the basis of computational results with superior success rate. In addition to new material discovery, structural optimization was achieved by BEAR,^[256–258] a Bayesian experimental autonomous researcher that leverages Bayesian optimization and autonomous high-throughput experimentation using robotic arms. The toughness of a type of

lattice structure was explored and optimized using a series of 3D-printers to iteratively build candidate prototypes based on the compression results. BEAR realized 60 times acceleration in identifying high-performing structures compared to a grid-based search.

4.3. Generative Designs

In addition to understanding the fundamental knowledge of biopolymer characteristics and fabrication process using various AI algorithms, novel biopolymer materials and bio-inspired designs can be actively optimized and generated to reach superior performance in chemical, mechanical, and biological properties. For instance,^[259] the concentration of a chitosan-agarose-gelatin biomaterial ink was optimized for its printing fidelity using the BO algorithm and the proposed concentration combination shows satisfactory performance in viscosity, hydrophilicity, degradability, and biological response. A similar optimization process has been applied to improve bio-inspired structures as well. For example, superior lattice structures with enhanced modulus and strength was obtained through a hybrid neural network and genetic optimization (NN-GO) adaptive method.^[260,261] The geometry of the lattice beam could be customized using Bézier curves to reduce high stress concentration profile. Furthermore, inspired from nature species, shark denticle bioinspired riblet structures were optimized using the response surface method to minimize the coefficient of drag.^[262] However, these applications usually perform optimization in the predefined design space. With the booming of generative AI algorithms, new techniques including generative adversarial networks (GANs), variational autoencoders (VAEs), and diffusion models have been applied to generate intricate bio-inspired designs using the latent space learned from data. Shen et al., utilized the Style-GAN algorithm to generate leaf-inspired unit cells with superior stiffness.^[263] The approach is able to generate infinite variant designs that are even outside the boundaries of the collected dataset, providing a unique way to explore broader design space. Besides, Chiu et al., designed bioinspired composite structures using conditional variational autoencoder (CVAE) to fulfill the desired stiffness and toughness with high efficiency (Figure 6D).^[264] Fracture toughness tests were performed to verify the performance of generated designs with good accuracy. Moreover, Lu et al., conducted graph-focused attention-based diffusion models and autoregressive transformer architectures to create spider-web inspired designs with heterogeneous hierarchical structures.^[265] The established framework has the potential to provide insights for fundamental biological understanding and meet with diverse design opportunities.

5. Challenges and Outlook

Industry and academic interests in biopolymers have grown due to their renewability, biodegradability, and customizable properties. Influenced by factors like composition and environment, biopolymers show promise in the biomedical, agricultural, and food sectors. They are expected to replace nonbiodegradable materials, though further research is needed on durability, performance, and life-cycle evaluation to support market expansion.

The primary research challenges in advancing biopolymer-related material systems for future development can be broadly summarized as developing rational design strategies that utilize the assembly and functionality of existing biopolymers with superior properties to enhance their performance.^[1,266] The first route is to leverage the functionality of natural nanofibers to develop biopolymer composites with improved performance. Natural fiber-reinforced biopolymers exhibit advantages like reduced weight, low cost, recyclability, and superior mechanical properties. However, they face challenges such as poor moisture resistance, dimensional stability, and limited fiber-polymer compatibility, which restrict potential applications, such as increased fiber content that enhances impact strength but raises brittleness and moisture absorption. Moreover, long-term properties like creep and fatigue behavior of natural fiber-reinforced biopolymers remain unclear. New approaches are needed to evaluate their performance throughout their lifespan, addressing compatibility and stability to broaden practical applications. Secondly, mimicking multiscale assemblies found in natural nanofibers (e.g., cellulose, chitin, and silk) also provides a promising route.^[267] By forming hierarchical structures, multiscale design can optimize the structure–property–function relationships. MD modeling can customize chemical structures, molecular weight, functional groups, and hydrophobicity/hydrophilicity, enabling priori predictions of nanofiber formation and assembly. At mesoscopic and macroscopic levels, nanofiber materials' mechanical, optical, and dynamic responses can be engineered through multiscale modeling integrated with experimental methods like spinning, film casting, and 3D printing. Introducing anisotropic nanofiber alignments and gradients enhances mechanical strength, flexibility, and dynamic interaction with environmental stimuli, such as humidity or temperature. Multiscale modeling can also predict deformation behavior for different nanofiber arrangements, while 3D printing enables site-specific construction of optimized structures.^[237] This rational approach is applicable throughout the entire design process, from molecular sequence to macroscopic manufacturing, promoting the realization of biopolymer materials with tailored properties and performance.

Multiscale modeling is crucial for designing and fabricating advanced biopolymer material systems, yet computational developments are still needed. First, the accuracy of modeling at all scales must be improved, for example, by developing more precise toolkits (e.g., forcefields, algorithms, and theories) to enhance the prediction of targeted functionalities.^[161,268,269] Second, balancing the required information and model resolution remains challenging. Generally, higher chemical specificity of models provides more detailed information about biopolymers. However, the connection to specific polymers becomes weaker when increasing the length and time scale. Nevertheless, large-scale predictions can capture broad polymer assembly reactions and dynamics.^[270] Third, bridging different scales in modeling is a pressing challenge, requiring advancements in both technical aspects and the integration of physics-based and data-driven approaches.^[271] Fourth, integration with experimental techniques remains underdeveloped. Further understanding of the structure–property–function relationships in natural materials will drive bioinspired strategies for the cost-effective design of novel biopolymer nanofiber-based functional

materials. These insights can be achieved through the synergistic integration of multiscale modeling with advanced static and dynamic characterization techniques, including electron microscopy, synchrotron sources, and ultrafast spectroscopy.^[272] However, discrepancies between modeling scales and experimental conditions continue to hinder effective coupling between simulation results and experimental data.

Although AI-driven techniques have been demonstrated in various applications including accurately predicting material characterization, optimizing fabrication processes, and generating bioinspired designs, challenges still remain in two major areas including data preparation and ML models. In specific, datasets for polymers, chemicals, and proteins play a crucial role in establishing foundations for large AI models and can serve as benchmarks within the communities.^[273,274] However, unlike typical materials and chemicals that have systemic representations and formats, bio-inspired designs usually have problem-specific settings and often require unique data collection and AI model choices. It remains a tough task to scale up AI approaches to these mechanics-related problems that have distinct design spaces, varied boundary conditions, and even different physics objectives (e.g., solid mechanics, fluid dynamics, and biological applications). Additionally, the existing datasets also face challenges from such as incomplete information and inconsistent data formats. For instance, data may originate from diverse sources, including computational simulations and experimental results. Building an accurate ML model requires more specific techniques and architectures. For example, multifidelity models, such as co-kriging methods, can be constructed using two datasets, each representing either low-fidelity or high-fidelity features. Co-kriging approach was successfully applied in developing a predictive model for polymer bandgaps with data from multiple sources including the Perdew–Burke–Ernzerhof (PBE) exchange-correlational functional (“low-fidelity”) and the Heyd–Scuseria–Ernzerhof (HSE06) functional (“high-fidelity”) of density functional theory.^[275] Their findings demonstrated not only improved performance compared to a single-fidelity Gaussian process method but also enhanced generalization capabilities for the model. Besides the mentioned approaches, active learning (i.e., reinforcement learning) and transfer learning (i.e., fine-tuning) can also be performed to mitigate the gap between predictive model trained on simulation dataset and physical experimental ground truth. Lastly, we have seen varying AI approaches to different tasks and applications such as graph-based methods on GENoME, and transformer-based methods on AlphaFold3.^[276] Leveraging the pretrained model for other related topics still requires more generalized AI models and thoughtful technical approaches.

Acknowledgements

X.Q.W. and Z.J. contributed equally to this work. This work was supported by the Barbara and Gerson Bakar Foundation, Department of Energy (Fund number: DE-EE0011181), and National Science Foundation (Fund number: DMR-2323731).

Conflict of Interest

The authors declare no conflict of interest.

Keywords

artificial intelligence, bioinspired materials, biopolymer, computational mechanics, machine learning, multiscale modeling

Received: November 3, 2024

Revised: January 24, 2025

Published online:

- [1] S. Ling, D. L. Kaplan, M. J. Buehler, *Nat. Rev. Mater.* **2018**, *3*, 1.
- [2] C. Liu, P. Luan, Q. Li, Z. Cheng, P. Xiang, D. Liu, Y. Hou, Y. Yang, H. Zhu, *Adv. Mater.* **2021**, *33*, 2001654.
- [3] J. L. Fredricks, A. M. Jimenez, P. Grandgeorge, R. Meidl, E. Law, J. Fan, E. Roumeli, *J. Polym. Sci.* **2023**, *61*, 2585.
- [4] Y. Pei, L. Wang, K. Tang, D. L. Kaplan, *Adv. Funct. Mater.* **2021**, *31*, 2008552.
- [5] A. Ghimire, Y.-Y. Tsai, P.-Y. Chen, S.-W. Chang, *Compos. Part. B-Eng.* **2021**, *215*, 108754.
- [6] A. Mtibe, M. P. Motloung, J. Bandyopadhyay, S. S. Ray, *Macromol. Rapid Commun.* **2021**, *42*, 2100130.
- [7] S. Hong, D. Sycks, H. F. Chan, S. Lin, G. P. Lopez, F. Guilak, K. W. Leong, X. Zhao, *Adv. Mater.* **2015**, *27*, 4035.
- [8] B. Shiroud Heidari, R. Ruan, E. Vahabli, P. Chen, E. M. De-Juan-Pardo, M. Zheng, B. Doyle, *Bioact. Mater.* **2023**, *19*, 179.
- [9] G. X. Gu, M. Takaffoli, M. J. Buehler, *Adv. Mater.* **2017**, *29*, 1700060.
- [10] P. R. Budarapu, X. Zhuang, T. Rabczuk, S. P. A. Bordase, *Adv. Appl. Mech.* **2019**, *52*, 1.
- [11] T. Magrini, A. Senol, R. Style, F. Bouville, A. R. Studart, *J. Mech. Phys. Solids* **2022**, *159*, 104750.
- [12] S. Ling, W. Chen, Y. Fan, K. Zheng, K. Jin, H. Yu, M. J. Buehler, D. L. Kaplan, *Prog. Polym. Sci.* **2018**, *85*, 1.
- [13] H. Moosavian, T. Tang, *J. Mech. Phys. Solids* **2024**, *192*, 105792.
- [14] P. N. Ciesielski, M. B. Pecha, A. M. Lattanzi, V. S. Bharadwaj, M. F. Crowley, L. Bu, J. V. Vermaas, K. X. Steirer, M. F. Crowley, *ACS Sustainable Chem. Eng.* **2020**, *8*, 3512.
- [15] Z. Wei, S. Wang, S. Farris, N. Chennuri, N. Wang, S. Shinsato, K. Demir, M. Horii, G. X. Gu, *Nat. Commun.* **2024**, *15*, 4337.
- [16] G. X. Gu, C.-T. Chen, D. J. Richmond, M. J. Buehler, *Mater. Horiz.* **2018**, *5*, 939.
- [17] K. Liu, R. Sun, C. Daraio, *Science* **2022**, *377*, 975.
- [18] B. G. Compton, J. A. Lewis, *Adv. Mater.* **2014**, *26*, 5930.
- [19] X. Sun, K. Zhou, F. Demoly, R. R. Zhao, H. J. Qi, *J. Appl. Mech.* **2024**, *91*, 030801.
- [20] J. Jung, A. Chen, G. X. Gu, *Mater. Today* **2024**, *73*, 1.
- [21] B. Ni, D. L. Kaplan, M. J. Buehler, *Chem* **2023**, *9*, 1828.
- [22] C. E. Athanasiou, X. Liu, H. Gao, *J. Appl. Mech.* **2024**, *91*, 110801.
- [23] Y. Kim, Y. Kim, C. Yang, K. Park, G. X. Gu, S. Ryu, *npj C. Mater.* **2021**, *7*, 140.
- [24] A. Pandey, W. Chen, S. Keten, *Commun. Mater.* **2024**, *5*, 83.
- [25] S. Kang, H. Song, H. S. Kang, B.-S. Bae, S. Ryu, *Mater. Des.* **2024**, *247*, 113377.
- [26] A. Pandey, E. Liu, J. Graham, W. Chen, S. Keten, *Patterns* **2023**, *4*, 100805.
- [27] S. Stoyanov, C. Bailey, in *2017 40th Int. Spring Seminar on Electronics Technology (ISSE)*, IEEE, Piscataway, NJ **2017**.
- [28] H. Liu, Z. Huang, S. S. Schoenholz, E. D. Cubuk, M. M. Smedskjaer, Y. Sun, W. Wang, M. Bauchy, *Mater. Horiz.* **2023**, *10*, 3416.
- [29] A. Masud, S. Nashar, S. A. Goraya, *Comput. Methods Appl. Mech. Eng.* **2023**, *417*, 116295.
- [30] B. Sanchez-Lengeling, A. Aspuru-Guzik, *Science* **2018**, *361*, 360.
- [31] G. M. Harshvardhan, M. K. Gourisaria, M. Pandey, S. S. Rautaray, *Comput. Sci. Rev.* **2020**, *38*, 100285.

[32] Z. Jin, Z. Zhang, K. Demir, G. X. Gu, *Matter* **2020**, *3*, 1541.

[33] M. Dijkstra, E. Luijten, *Nat. Mater.* **2021**, *20*, 762.

[34] Z. Jin, Z. Zhang, J. Ott, G. X. Gu, *Addit. Manuf.* **2021**, *37*, 101696.

[35] X. Y. Lee, S. K. Saha, S. Sarkar, B. Giera, *Addit. Manuf.* **2020**, *36*, 101444.

[36] Y. Gao, D. Zhou, J. Lyu, A. Sigen, Q. Xu, B. Newland, K. Matyjaszewski, H. Tai, W. Wang, *Nat. Rev. Chem.* **2020**, *4*, 194.

[37] Y. Pei, L. Wang, K. Tang, D. L. Kaplan, *Adv. Funct. Mater.* **2021**, *31*, 2008552.

[38] E. Baer, A. Hiltner, H. D. Keith, *Science* **1987**, *235*, 1015.

[39] M. S. Ganewatta, Z. Wang, C. Tang, *Nat. Rev. Chem.* **2021**, *5*, 753.

[40] Y. Sun, Y. Bai, W. Yang, K. Bu, S. K. Tanveer, J. Hai, *Front. Chem.* **2022**, *10*, 915648.

[41] S. S. A. P. RG, G. Bajaj, A. E. John, S. Chandran, V. V. Kumar, S. Ramakrishna, *J. Mater. Sci.: Mater. Med.* **2023**, *34*, 162.

[42] R. Kalpana Manivannan, N. Sharma, V. Kumar, I. Jayaraj, S. Vimal, M. Umesh, *Carbohydr. Polym. Technol. Appl.* **2024**, *8*, 100536.

[43] A. Goeppert, M. Czaun, G. K. Surya Prakash, G. A. Olah, *Energy Environ. Sci.* **2012**, *5*, 7833.

[44] P. C. Srinivasa, R. N. Tharanathan, *Food Rev. Int.* **2007**, *23*, 53.

[45] C. Lorenz, S. Köster, *Biophys. Rev.* **2022**, *3*, 31304.

[46] A. S. A. Mohammed, M. Naveed, N. Jost, *J. Polym. Environ.* **2021**, *29*, 2359.

[47] C. M. Runnels, K. A. Lanier, J. K. Williams, J. C. Bowman, A. S. Petrov, N. V. Hud, L. D. Williams, *J. Mol. Evol.* **2018**, *86*, 598.

[48] A. N. Nekrasov, Y. P. Kozmin, S. V. Kozyrev, N. G. Esipova, R. H. Ziganшин, A. A. Anashkina, *Biophysics* **2020**, *65*, 907.

[49] Y. Sang, M. Liu, *Chem. Sci.* **2022**, *13*, 633.

[50] Y. Loo, M. Goktas, A. B. Tekinay, M. O. Guler, C. A. E. Hauser, A. Mitraki, *Adv. Healthcare Mater.* **2015**, *4*, 2557.

[51] Z. Wang, Y. Shang, H. Luo, C. Yang, Z. Yang, C. Ren, J. Liu, *Nanoscale* **2023**, *15*, 7502.

[52] C. Yuan, W. Ji, R. Xing, J. Li, E. Gazit, X. Yan, *Nat. Rev. Chem.* **2019**, *3*, 567.

[53] A. C. Engler, A. Shukla, S. Puranam, H. G. Buss, N. Jreige, P. T. Hammond, *Biomacromolecules* **2011**, *12*, 1666.

[54] K. A. Henzler-Wildman, M. Lei, V. Thai, S. J Kerns, M. Karplus, D. Kern, *Nature* **2007**, *450*, 913.

[55] X. Du, Y. Li, Y.-L. Xia, S.-M. Ai, J. Liang, P. Sang, X.-L. Ji, S.-Q. Liu, *Int. J. Mol. Sci.* **2016**, *17*, 144.

[56] S. R. Tzeng, C. G. Kalodimos, *Nature* **2009**, *462*, 368.

[57] X. Liu, M. Zheng, X. Wang, X. Luo, M. Hou, O. Yue, *ACS Biomater. Sci. Eng.* **2020**, *6*, 739.

[58] A. Gautieri, S. Vesentini, A. Redaelli, M. J. Buehler, *Nano Lett.* **2011**, *11*, 757.

[59] P. Fratzl, *Collagen: Structure and Mechanics, an Introduction*, Springer, Boston, MA, United States **2008**.

[60] D. M. Darvish, *Mater. Today Bio* **2022**, *15*, 100322.

[61] A. Vijayalekha, S. K. Anandasadagopan, A. K. Pandurangan, *Appl. Biochem. Biotechnol.* **2023**, *195*, 4617.

[62] J. Yang, H. Wang, Y. Zhou, L. Duan, K. H. Schneider, Z. Zheng, F. Han, X. Wang, G. Li, *Macromol. Biosci.* **2023**, *23*, 2300105.

[63] S. Yang, C. Zhao, Y. Yang, J. Ren, S. Ling, *ACS Nano* **2023**, *17*, 7662.

[64] J. Chen, J. Liu, W. Yang, Y. Pei, *Polymers* **2023**, *15*, 375.

[65] L. Zhang, W. Zhang, Y. Hu, Y. Fei, H. Liu, Z. Huang, C. Wang, D. Ruan, B. C. Heng, W. Chen, W. Shen, *ACS Biomater. Sci. Eng.* **2021**, *817*.

[66] T. P. Nguyen, Q. V. Nguyen, V.-H. Nguyen, T.-H. Le, V. Q. N. Huynh, D.-V. N. Vo, Q. T. Trinh, S. Y. Kim, Q. V. Le, *Polymers* **2019**, *11*, 1933.

[67] M. Delbianco, P. H. Seeberger, *Mater. Horiz.* **2020**, *7*, 963.

[68] G. Yang, W. Zheng, G. Tao, L. Wu, Q.-F. Zhou, Z. Kochovski, T. Ji, H. Chen, X. Li, Y. Lu, H.-M. Ding, H.-B. Yang, G. Chen, M. Jiang, *ACS Nano* **2019**, *13*, 13474.

[69] F. Khan, D. Walsh, A. J. Patil, A. W. Perriman, S. Mann, *Soft Matter* **2009**, *5*, 3081.

[70] G. Eggleston, J. P. Doyle, *ACS Symp. Ser.* **2006**, *935*, 19.

[71] P. Sukhavattanakul, P. Pisitsak, S. Ummartyotin, R. Narain, *Macromol. Biosci.* **2023**, *23*, 2200372.

[72] N. Jabeen, M. Atif, *Polym. Adv. Technol.* **2024**, *35*, e6203.

[73] A. Plucinski, Z. Lyu, B. V. K. J. Schmidt, *J. Mater. Chem. B* **2021**, *9*, 7030.

[74] L. Jojo, D. Goswami, S. Babu, A. Singh, V. Krishnan, B. Thomas, in *Handbook of Biomass*, Springer, Singapore **2024**, pp. 809–854.

[75] J. A. Patterson, M. J. Emes, I. J. Tetlow, *Encyclopedia of Appl. Plant Sci.* **2017**, *1*, 570.

[76] C.-Y. Su, D. Li, L.-J. Wang, Y. Wang, *Crit. Rev. Food Sci. Nutr.* **2023**, *63*, 6923.

[77] M. Salimi, B.-E. Channab, A. El Idrissi, M. Zahouily, E. Motamedi, *Carbohydr. Polym.* **2023**, *322*, 121326.

[78] R. Abka-khajouei, L. Tounsi, N. Shahabi, A. K. Patel, S. Abdelkafi, P. Michaud, *Marine Drugs* **2022**, *20*, 364.

[79] K. Y. Lee, D. J. Mooney, *Prog. Polym. Sci.* **2012**, *37*, 106.

[80] C. Li, J. Wu, H. Shi, Z. Xia, J. K. Sahoo, J. Yeo, D. L. Kaplan, *Adv. Mater.* **2022**, *34*, 2105196.

[81] F. J. Martin-Martinez, *Proc. Natl. Acad. Sci. USA* **2018**, *115*, 7174.

[82] B.-E. Channab, A. El Idrissi, Y. Essamlali, M. Zahouily, *J. Environ. Manag.* **2024**, *352*, 119928.

[83] M. Nero, H. Ali, Y. Li, T. Willhammar, *Small Methods* **2024**, *8*, 2301304.

[84] Z. Wu, S. Chen, J. Li, B. Wang, M. Jin, Q. Liang, D. Zhang, Z. Han, L. Deng, X. Qu, H. Wang, *Adv. Funct. Mater.* **2023**, *33*, 2214327.

[85] D. J. Cosgrove, *Nat. Rev. Mol. Cell Biol.* **2023**, *25*, 340.

[86] L. Bai, L. Liu, M. Esquivel, B. L. Tardy, S. Huan, X. Niu, S. Liu, G. Yang, Y. Fan, O. J. Rojas, *Chem. Rev.* **2022**, *122*, 11604.

[87] F. Yuan, X.-X. Zhang, K. Wu, Z. Li, Y. Lin, X. Liang, Q. Yang, T. Liu, *Cell Rep. Phys. Sci.* **2023**, *4*, 101644.

[88] S. Sviben, O. Spaeker, M. Bennet, M. Albéric, J.-H. Dirks, B. Moussian, P. Fratzl, L. Bertinetti, Y. Politi, *ACS Appl. Mater. Interfaces* **2020**, *12*, 25581.

[89] G. Ali, M. Sharma, E.-S. Salama, Z. Ling, X. Li, *Biomass Convers. Biorefinery* **2022**, *14*, 4567.

[90] D. N. Carvalho, C. Gonçalves, R. O. Sousa, R. L. Reis, J. M. Oliveira, T. H. Silva, *Mar. Biotechnol.* **2024**, *26*, 1079.

[91] M. J. Getahun, B. B. Kassie, T. S. Alemu, *Process Biochem.* **2024**, *145*, 261.

[92] E. J. Cha, D. S. Lee, H. Kim, Y. H. Kim, B. G. Kim, Y. Yoo, Y. S. Kim, D.-G. Kim, *RSC Adv.* **2019**, *9*, 15780.

[93] A. Samir, F. H. Ashour, A. A. Hakim, M. Bassyouni, *npj Mater. Degrad.* **2022**, *6*, 68.

[94] S. Shah, A. Kumar, *Eur. J. Environ. Sci.* **2020**, *10*, 76.

[95] S. Shaikh, M. Yaqoob, P. Aggarwal, *Curr. Res. Food Sci.* **2021**, *4*, 503.

[96] E. Malikmammadov, T. E. Tanir, A. Kiziltay, V. Hasirci, N. Hasirci, *Polym. Ed.* **2018**, *29*, 863.

[97] T. K. Dash, V. B. Konkimalla, *Mol. Pharmaceutics* **2012**, *9*, 2365.

[98] K. Matyjaszewski, *Prog. Polym. Sci.* **2005**, *30*, 858.

[99] O. Ikkala, G. ten Brinke, *Chem. Commun.* **2004**, 2131.

[100] C. Chen, Z. J. Wang, H. Lu, Y. Zhao, Z. Shi, *Nat. Commun.* **2021**, *12*, 4526.

[101] N. A. Lynd, A. J. Meuler, M. A. Hillmyer, *Prog. Polym. Sci.* **2008**, *33*, 875.

[102] I. A. O. Beeren, F. L. C. Morgan, T. Rademakers, J. Bauer, P. J. Dijkstra, L. Moroni, M. B. Baker, *J. Am. Chem. Soc.* **2024**, *146*, 24330.

[103] A.-V. Ruzette, L. Leibler, *Nat. Mater.* **2005**, *4*, 19.

[104] A.-S. Glaive, C. L. Cour, J.-M. Guigner, C. Amiel, G. Volet, *Langmuir* **2024**, *40*, 2050.

[105] C. T. Huynh, M. K. Nguyen, D. S. Lee, *Macromolecules* **2011**, *44*, 6629.

[106] S. Nambiar, J. T. W. Yeow, *Biosens. Bioelectron.* **2011**, *26*, 1825.

[107] H.-M. Kang, Y.-L. Cai, P.-S. Liu, *Carbohydr. Res.* **2006**, *341*, 2851.

[108] E. Alipour, S. Norouzi, H. Yousefzadeh, R. Mohammadi, M. S. Amini-Fazl, *J. Mater. Sci.: Mater. Electron.* **2021**, *32*, 24812.

[109] S. Fatullayeva, D. Tagiyev, N. Zeynalov, S. Mammadova, E. Aliyeva, *J. Polym. Res.* **2022**, *29*, 259.

[110] Q. Luo, H. Gao, L. Peng, G. Liu, Z. Zhang, *J. Appl. Polym. Sci.* **2016**, *133*, 43465.

[111] A. Das, A. Babu, S. Chakraborty, J. F. R. Van Guyse, R. Hoogenboom, S. Maji, *Adv. Funct. Mater.* **2024**, *34*, 2402432.

[112] Z. Tang, T. Okano, *Regener. Biomater.* **2014**, *1*, 91.

[113] P. T. Benavides, U. Lee, O. Zarè-Mehrjerdi, *J. Cleaner Prod.* **2020**, *277*, 124010.

[114] E. Castro-Aguirre, F. Iñiguez-Franco, H. Samsudin, X. Fang, R. Auras, *Adv. Drug Delivery Rev.* **2016**, *107*, 333.

[115] T. A. Hottle, M. M. Bilec, A. E. Landis, *Polym. Degrad. Stab.* **2013**, *98*, 1898.

[116] K. Madhavan Nampoothiri, N. R. Nair, R. P. John, *Bioresour. Technol.* **2010**, *101*, 8493.

[117] M. Guicherd, M. Ben Khaled, M. Guérout, J. Nomme, M. Dalibey, F. Grimaud, P. Alvarez, E. Kamionka, S. Gavalda, M. Noël, M. Vuillemin, E. Amillastre, D. Labourdette, G. Cioci, V. Tournier, V. Kitpreechavanich, P. Dubois, I. André, S. Duquesne, A. Marty, *Nature* **2024**, *631*, 884.

[118] A. Chamas, et al., *ACS Sustainable Chem. Eng.* **2020**, *8*, 3494.

[119] V. Rajgond, A. Mohite, N. More, A. More, *Polym. Bull.* **2023**, *81*, 5703.

[120] B. Guo, L. Glavas, A.-C. Albertsson, *Prog. Polym. Sci.* **2013**, *38*, 1263.

[121] M. Zarei, G. Lee, S. G. Lee, K. Cho, *Adv. Mater.* **2023**, *35*, 2203193.

[122] S. A. Hollingsworth, R. O. Dror, *Neuron* **2018**, *99*, 1129.

[123] S. Plimpton, *J. Comput. Phys.* **1995**, *117*, 1.

[124] K. Hyltegren, M. Polimeni, M. Slepö, M. Lund, *J. Chem. Theory Comput.* **2020**, *16*, 1843.

[125] W. Xia, L. A. R. Pestana, *Fundamentals of Multiscale Modeling of Structural Materials*, Elsevier, Cambridge, MA, United States **2023**.

[126] S. Dhamankar, M. A. Webb, *J. Polym. Sci.* **2021**, *59*, 2613.

[127] S. Berend, B. Smit, P. A. J. Hilbers, K. Esselink, L. A. M. Rupert, N. M. Van Os, A. G. Schlijper, *J. Phys. Chem.* **1991**, *95*, 6361.

[128] F. Daan, S. Berend, *Understanding Molecular Simulation: from Algorithms to Applications*, Elsevier, San Diego, CA, United States **2023**.

[129] P. Españo, P. B. Warren, *J. Chem. Phys.* **2017**, *146*, 150901.

[130] X. Wu, B. R. Brooks, *Chem. Phys. Lett.* **2003**, *381*, 512.

[131] G. A. Huber, J. A. McCammon, *Trends Chem.* **2019**, *1*, 727.

[132] A. Vitalis, R. V. Pappu, *Ann. Rep. in Comput. Chem.* **2009**, *5*, 49.

[133] C. Z. Mooney, *Monte Carlo Simulation*, Sage, Thousand Oaks, CA, United States, **1997**.

[134] W. M. Mark, *Soft Matter* **2007**, *1*, 87.

[135] E. Engel, *Density Functional Theory*, Springer-Verlag Berlin, Germany **2011**.

[136] D. Zhao, X. Q. Wang, L.-H. Tam, C. L. Chow, D. Lau, *Thin-Walled Struct.* **2024**, *196*, 111536.

[137] R. W. Pastor, A. D. MacKerell, *J. Phys. Chem. Lett.* **2011**, *2*, 1526.

[138] M. Wohlert, T. Benselelt, L. Wågberg, I. Furó, L. A. Berglund, J. Wohlert, *Cellulose* **2022**, *29*, 1.

[139] A. Y. Mehandzhiyski, I. Zozoulenko, *Polysaccharides* **2021**, *2*, 257.

[140] Y. Zhang, H. He, Y. Liu, Y. Wang, F. Huo, M. Fan, H. Adidharma, X. Li, S. Zhang, *Green Chem.* **2019**, *21*, 9.

[141] S. Keten, Z. Xu, B. Ihle, M. J. Buehler, *Nat. Mater.* **2010**, *9*, 359.

[142] D. Nepal, S. Kang, K. M. Adstedt, K. Kanhaiya, M. R. Bockstaller, L. C Brinson, M. J. Buehler, P. V. Coveney, K. Dayal, J. A. El-Awady, L. C. Henderson, D. L. Kaplan, S. Keten, N. A. Kotov, G. C. Schatz, S. Vignolini, F. Vollrath, Y. Wang, B. I. Yakobson, V. V. Tsukruk, H. Heinz, *Nat. Mater.* **2023**, *22*, 18.

[143] S. W. Cranford, A. Tarakanova, N. M. Pugno, M. J. Buehler, *Nature* **2012**, *482*, 72.

[144] P. Batys, D. Fedorov, P. Mohammadi, L. Lemetti, M. B. Linder, M. Sammalkorpi, *Biomacromolecules* **2021**, *22*, 690.

[145] D. A. Tolmachev, M. Malkamäki, M. B. Linder, M. Sammalkorpi, *Biomacromolecules* **2023**, *24*, 5638.

[146] A. Tarakanova, W. Huang, Z. Qin, D. L. Kaplan, M. J. Buehler, *ACS Biomater. Sci. Eng.* **2017**, *3*, 2889.

[147] E. C. Joshua, B. M. Tyler, J. Arthi, *Soft Matter* **2017**, *13*, 2907.

[148] A. Prhashanna, P. A. Taylor, J. Qin, K. L. Kiick, A. Jayaraman, *Biomacromolecules* **2019**, *20*, 1178.

[149] M. Milazzo, A. David, G. S. Jung, S. Danti, M. J. Buehler, *Biomater. Sci.* **2021**, *9*, 3390.

[150] A. K. Nair, A. Gautieri, S.-W. Chang, M. J. Buehler, *Nat. Commun.* **2013**, *4*, 1.

[151] A. L. Harmat, M. Morga, J. L. Lutkenhaus, P. Batys, M. Sammalkorpi, *Appl. Surf. Sci.* **2023**, *615*, 156331.

[152] D. Tolmachev, N. Lukasheva, G. Mamistvalov, M. Karttunen, *Polymers* **2020**, *12*, 1279.

[153] A. P. Paavo, P. Antti, A. K. Jukka, *Carbohydr. Polym.* **2021**, *251*, 117064.

[154] M. Karim, C. Landry, *Cellulose* **2012**, *19*, 337.

[155] H. Jaroslav, M. Karim, *Biopolymers* **2006**, *82*, 59.

[156] N. Zhang, *Modell. Simul. Mater. Sci. Eng.* **2015**, *23*, 085010.

[157] K. Jin, Z. Qin, M. J. Buehler, *J. Mech. Behav. Biomed. Mater.* **2015**, *42*, 198.

[158] C. Landry, M. Karim, *J. Phys. Chem. B* **2012**, *116*, 4163.

[159] T. D. Potter, J. Tasche, M. R. Wilson, *Phys. Chem. Chem. Phys.* **2019**, *21*, 1912.

[160] Z. Jarin, J. Newhouse, G. A. Voth, *J. Chem. Theory Comput.* **2021**, *17*, 1170.

[161] J. Jin, A. J. Pak, A. E. P. Durumeric, T. D. Loose, G. A. Voth, *J. Chem. Theory Comput.* **2022**, *18*, 5759.

[162] S. Kmiecik, D. Gront, M. Kolinski, L. Wieteska, A. E. Dawid, A. Kolinski, *Chem. Rev.* **2016**, *116*, 7898.

[163] C. Arnarez, J. J. Uusitalo, M. F. Masman, H. I. Ingólfsson, D. H. de Jong, M. N. Melo, X. Periole, A. H. de Vries, S. J. Marrink, *J. Chem. Theory Comput.* **2015**, *11*, 260.

[164] P. C. T. Souza, R. Alessandri, J. Barnoud, S. Thallmair, I. Faustino, F. Grünewald, I. Patmanidis, H. Abdizadeh, B. M. H. Bruininks, T. A. Wassenaar, P. C. Kroon, J. Melcr, V. Nieto, V. Corradi, H. M. Khan, J. Domanski, M. Javanainen, H. Martinez-Seara, N. Reuter, R. B. Best, I. Vattulainen, L. Monticelli, X. Periole, D. P Tieleman, A. H. de Vries, S. J. Marrink, *Nat. Methods* **2021**, *18*, 382.

[165] A. Gousssem, R. Mbarki, F. Al Khatib, M. Adouni, *Bioengineering* **2022**, *9*, 193.

[166] A. F. Ghobadi, A. Jayaraman, *Soft Matter* **2016**, *12*, 2276.

[167] E. C. Joshua, J. Arthi, *Soft Matter* **2017**, *13*, 6770.

[168] K. Mateusz, K. Andrzej, K. Sebastian, *J. Chem. Theory Comput.* **2014**, *10*, 2224.

[169] C. Y. Chen, F. A. Escobedo, *Langmuir: ACS J. Surf. Colloids* **2020**, *36*, 5754.

[170] A. E. Hafner, N. G. Gyori, C. A. Bench, L. K. Davis, A. Saric, *Biophys. J.* **2020**, *119*, 1791.

[171] V. Maisa, M. Jukka, S. Maria, *J. Phys. Chem. B* **2018**, *122*, 4851.

[172] A. Tarakanova, J. Ozsvár, A. S. Weiss, M. J. Buehler, *Mater. Today Bio* **2019**, *3*, 100016.

[173] L. K. Davis, A. Saric, B. W. Hoogenboom, A. Zilman, *Biophys. J.* **2021**, *120*, 1565.

[174] Z. Adamczyk, *Curr. Opin. Colloid Interface Sci.* **2012**, *17*, 173.

[175] L. Li, P. Pérré, X. Frank, K. Mazeau, *Carbohydr. Polym.* **2015**, *127*, 438.

[176] D. C. Adler, M. J. Buehler, *Soft Matter* **2013**, *9*, 7138.

[177] Y. Mai, A. Eisenberg, *Chem. Soc. Rev.* **2012**, *41*, 5969.

[178] M. Junlin, J. Mai, D. Sun, L. Li, J. Zhou, *J. Chem. Eng. Data* **2016**, *61*, 3998.

[179] S. Lin, S. Ryu, O. Tokareva, G. Gronau, M. M. Jacobsen, W. Huang, D. J. Rizzo, D. Li, C. Staii, N. M. Pugno, J. Y. Wong, D. L. Kaplan, M. J. Buehler, *Nat. Commun.* **2015**, *6*, 1.

[180] Z. Zhuang, T. Jiang, J. Lin, L. Gao, C. Yang, L. Wang, C. Cai, *Angew. Chem., Int. Ed.* **2016**, *55*, 12522.

[181] Y. Li, X. Zhang, D. Cao, *Sci. Rep.* **2013**, *3*, 3271.

[182] A. A. Gavrilov, *J. Chem. Phys.* **2020**, *152*, 164101.

[183] K. P. Emanuel, L. Kirill, V. P. Igor, *Phys. Chem. Chem. Phys.* **2015**, *17*, 24452.

[184] A. A. Gavrilov, A. V. Chertovich, E. Y. Kramarenko, *J. Chem. Phys.* **2016**, *145*.

[185] A. Argun, A. Callegari, G. Volpe, *Simulation of Complex Systems*, IOP Publishing, Bristol, UK **2021**.

[186] A. Muñiz-Chicharro, L. W. Yotapka, R. E. Amaro, R. C. Wade, W. Interdiscip, *Rev. Comput. Mol. Sci.* **2023**, *13*, e1649.

[187] H. Kang, P. A. Pincus, C. Hyeon, D. Thirumalai, *Phys. Rev. Lett.* **2015**, *114*, 068303.

[188] A. F. Ghobadi, A. Jayaraman, *J. Phys. Chem. B* **2016**, *120*, 9788.

[189] A. Statt, H. Casademunt, C. P. Brangwynne, A. Z. Panagiotopoulos, *J. Chem. Phys.* **2020**, *152*, 075101.

[190] L. D. Cairano, S. Benjamin, C. Vania, *Biophys. J.* **2021**, *120*, 4722.

[191] C. Shen, C.-R. Qin, T.-L. Xu, K. Chen, W.-D. Tian, *Soft Matter* **2022**, *18*, 1489.

[192] B. Gong, X. Wei, J. Qian, Y. Lin, *ACS Biomater. Sci. Eng.* **2019**, *5*, 3720.

[193] A. M. Walczak, J. M. Antosiewicz, *Phys. Rev. E* **2002**, *66*, 051911.

[194] P. M. Blanco, J. L. Garcés, S. Madurga, F. Mas, *Soft Matter* **2018**, *14*, 3105.

[195] L. Lemetti, A. Scacchi, Y. Yin, M. Shen, M. B. Linder, M. Sammalkorpi, A. S. Aranko, *Biomacromolecules* **2022**, *23*, 3142.

[196] Z. Emiko, A.-K. Alfredo, E. Zumbro, A. Alexander-Katz, *PLoS One* **2021**, *16*, 0245405.

[197] B. S. Hanson, L. Dougan, *Biomacromolecules* **2021**, *22*, 4191.

[198] P. Mereghetti, R. R. Gabdoulline, R. C. Wade, *Biophys. J.* **2010**, *99*, 3782.

[199] P. Mereghetti, R. C. Wade, *J. Phys. Chem. B* **2012**, *116*, 8523.

[200] M. I. Ioana, K. D. O. Wouter, J. B. Wim, *J. Chem. Phys.* **2016**, *144*.

[201] D. Maciej, T. Joanna, *BMC Biophys.* **2011**, *4*, 1.

[202] A. Mie, P. Chiara, R. Karsten, *Front. Chem.* **2019**, *7*, 434159.

[203] O. Ronaldo Junio De, *J. Chem. Phys.* **2018**, *149*.

[204] A. Saric, Y. C. Chebaro, T. P. J. Knowles, D. Frenkel, *Proc. Natl. Acad. Sci. USA* **2014**, *111*, 17869.

[205] Z. Toprakcioglu, A. Kamada, T. C. Michaels, M. Xie, J. Krausser, J. Wei, A. Saric, M. Vendruscolo, T. P. J. Knowles, *Proc. Natl. Acad. Sci. USA* **2022**, *119*, 2109718119.

[206] K. Johannes, P. J. K. Tuomas, E. Š. Andela, *Proc. Natl. Acad. Sci. USA* **2020**, *117*, 33090.

[207] T. C. T. Michaels, A. Saric, S. Curk, K. Bernfur, P. Arosio, G. Meisl, A. J. Dear, S. I. A. Cohen, C. M. Dobson, M. Vendruscolo, S. Linse, T. P. J. Knowles, *Nat. Chem.* **2020**, *12*, 445.

[208] U. Rana, C. P. Brangwynne, A. Z. Panagiotopoulos, *J. Chem. Phys.* **2021**, *155*.

[209] S. Das, A. Eisen, Y.-H. Lin, H. S. Chan, *J. Phys. Chem. B* **2018**, *122*, 5418.

[210] T. K. Lytle, M. Radhakrishna, C. E. Sing, *Macromolecules* **2016**, *49*, 9693.

[211] M.-T. Wei, S. Elbaum-Garfinkle, A. S. Holehouse, C. C.-H. Chen, M. Feric, C. B. Arnold, R. D. Priestley, R. V. Pappu, C. P. Brangwynne, *Nat. Chem.* **2017**, *9*, 1118.

[212] D. Kosior, M. Morgia, P. Maroni, M. Cieśla, Z. Adamczyk, *J. Phys. Chem. C* **2020**, *124*, 4571.

[213] P. Y. Chew, A. Reinhardt, *J. Chem. Phys.* **2023**, *158*, 30902.

[214] K. Wong, R. Qi, Y. Yang, Z. Luo, S. Guldin, K. T. Butler, *JACS Au* **2024**, *4*, 3492.

[215] A. M. Watkins, C. Geniesse, W. Kladwang, P. Zakrevsky, L. Jaeger, R. Das, *Sci. Adv.* **2018**, *4*, eaar5316.

[216] U. K. Jaeup, Y. Y. Biao, L. W. Bo, *Macromolecules* **2012**, *45*, 3263.

[217] W. Li, Y. X. Liu, *J. Chem. Phys.* **2021**, *154*.

[218] A. Ianiro, H. Wu, M. M. J. van Rijt, M. P. Vena, A. D. A. Keizer, A. C. C. Esteves, R. Tuinier, H. Friedrich, N. A. J. M. Sommerdijk, J. P. Patterson, *Nat. Chem.* **2019**, *11*, 320.

[219] R. Ettelaie, A. Akinshina, E. Dickinson, *Faraday Discuss.* **2008**, *139*, 161.

[220] P. Chen, K. D. Dorfman, *Proc. Natl. Acad. Sci. USA* **2023**, *120*, 2308698120.

[221] A. Scacchi, M. Sammalkorpi, T. Ala-Nissila, *J. Chem. Phys.* **2021**, *155*.

[222] A. Scacchi, S. J. Nikkhah, M. Sammalkorpi, T. Ala-Nissila, *Phys. Rev. Res.* **2021**, *3*, L022008.

[223] A. J. Archer, A. M. Rucklidge, E. Knobloch, *Phys. Rev. Lett.* **2013**, *111*, 165501.

[224] A. J. Archer, A. M. Rucklidge, E. Knobloch, *Phys. Rev. E – Statistical, Nonlinear, Soft Matter Phys.* **2015**, *92*, 012324.

[225] S. Angioletti-Uberti, M. Ballauff, J. Dzubiella, *Soft Matter* **2014**, *10*, 7932.

[226] H. Tan, M. Zhang, Y. Deng, Q. Song, D. Yan, *Polymer* **2013**, *54*, 6853.

[227] M. C. Bott, J. M. Brader, *Phys. Rev. E* **2016**, *94*, 012603.

[228] A. Böbel, M. C. Bott, H. Modest, J. M. Brader, C. Räth, *New J. Phys.* **2019**, *21*, 013031.

[229] D. J. Gardiner, P. R. Graves, *Practical Raman Spectroscopy*, **1989**, Practical Raman Spectroscopy.

[230] B. Gieroba, G. Kalisz, M. Krysa, M. Khalavka, A. Przekora, *Int. J. Mol. Sci.* **2023**, *24*, 2630.

[231] C. W. Oatley, J. A. Soc., *J. Appl. Phys.* **1982**, *53*, R1.

[232] G. Binnig, C. F. Quate, C. Gerber, *Phys. Rev. Lett.* **1986**, *56*, 930.

[233] E. K. Oikonomou, J.-F. Berret, *Materials* **2021**, *14*, 5749.

[234] A. Akbarzadeh Solbu, A. Koernig, J. S. Kjesbu, D. Zaytseva-Zotova, M. Sletmoen, B. L. Strand, *Carbohydr. Polym.* **2022**, *276*, 118804.

[235] B. Pan, *Exp. Mech.* **2011**, *51*, 1223.

[236] M. Liu, J. Guo, C.-Y. Hui, A. T. Zehnder, *Exp. Mech.* **2019**, *59*, 1021.

[237] C. Zhu, *Adv. Mater.* **2024**, *36*, 2314204.

[238] M. A. Skylar-Scott, J. Mueller, C. W. Visser, J. A. Lewis, *Nature* **2019**, *575*, 330.

[239] N. Li, D. Qiao, S. Zhao, Q. Lin, B. Zhang, F. Xie, *Mater. Today Chem.* **2021**, *20*, 100459.

[240] L. Himanen, A. Geurts, A. S. Foster, P. Rinke, *Adv. Sci.* **2019**, *6*, 1900808.

[241] C. Kuenneth, J. Lalonde, B. L. Marrone, C. N. Iverson, R. Ramprasad, G. Pilania, *Commun. Mater.* **2022**, *3*, 1.

[242] D. Martí, R. Pétyua, E. Bosoni, A.-C. Dublanchet, S. Mohr, F. Léonforte, *ACS Appl. Polym. Mater.* **2024**, *6*, 4449.

[243] H. Moriwaki, Y.-S. Tian, N. Kawashita, T. Takagi, *J. Cheminform.* **2018**, *10*, 4.

[244] C. Xu, Y. Wang, A. B. Farimani, *npj Comput. Mater.* **2023**, *9*, 64.

[245] C. Kuenneth, R. Ramprasad, *Nat. Commun.* **2023**, *14*, 1.

[246] Z. Jin, Z. Zhang, G. X. Gu, *Manuf. Lett.* **2019**, *22*, 11.

[247] F. María, C. Patricia, V. Manuel, *Polymers* **2023**, *15*, 641.

[248] L. Yang, Z. Qin, *Cell Rep. Phys. Sci.* **2023**, *4*, 101424.

[249] D. Thomas, M. S. Nath, N. Mathew, R. Reshma, E. Philip, M. S. Latha, *J. Drug Deliv. Sci. Technol.* **2020**, *59*, 101894.

[250] H. Su, K.-Y. Liu, A. Karydis, D. G. Abebe, C. Wu, K. M. Anderson, N. Ghadri, P. Adatrow, T. Fujiwara, J. D. Bumgardner, *Biomed. Mater.* **2016**, *12*, 015003.

[251] C. Weerapoprasit, J. Prachayawarakorn, *Polym. Compos.* **2016**, *37*, 3365.

[252] Z. Jin, Z. Zhang, X. Shao, G. X. Gu, *ACS Biomater. Sci. Eng.* **2023**, *9*, 3945.

[253] J. M. Bone, C. M. Childs, A. Menon, B. Póczos, A. W. Feinberg, P. R. LeDuc, N. R. Washburn, *ACS Biomater. Sci. Eng.* **2020**, *6*, 7021.

[254] B. Jyotisman, M. Chandrasekaran, *Multiscale Multidiscipl. Model. Exp. Des.* **2024**, 7, 4487.

[255] A. H. Etefagh, M. R. Razfar, *Proc. Inst. Mech. Eng. Part B: J. Eng. Manuf.* **2024**, 238, 1448.

[256] N. J. Szymanski, B. Rendy, Y. Fei, R. E. Kumar, T. He, D. Milsted, M. J. McDermott, M. Gallant, E. D. Cubuk, A. Merchant, H. Kim, A. Jain, C. J. Bartel, K. Persson, Y. Zeng, G. Ceder, *Nature* **2023**, 624, 86.

[257] A. E. Gongora, B. Xu, W. Perry, C. Okoye, P. Riley, K. G. Reyes, E. F. Morgan, K. A. Brown, *Sci. Adv.* **2020**, 6, eaaz1708.

[258] K. L. Snapp, B. Verdier, A. E. Gongora, S. Silverman, A. D. Adesiji, E. F. Morgan, T. J. Lawton, E. Whiting, K. A. Brown, *Nat. Commun.* **2024**, 15, 4290.

[259] A. Hashemi, M. Ezati, I. Zumberg, T. Vicar, L. Chmelikova, V. Cmiel, V. Provaznik, *Mater. Today Commun.* **2024**, 40, 109777.

[260] S. Lee, Z. Zhang, G. X. Gu, *Mater. Horiz.* **2022**, 9, 952.

[261] S. Lee, Z. Zhang, G. X. Gu, *ACS Appl. Mater. Interfaces* **2023**, 15, 22543.

[262] W. Li, J. Ott, M. Lazalde, G. X. Gu, *Bioinspir. Biomim.* **2020**, 15, 026001.

[263] S. C. Y. Shen, M. J. Buehler, *Commun. Eng.* **2022**, 1, 37.

[264] Y.-H. Chiu, Y.-H. Liao, J.-Y. Juang, *Polymers* **2023**, 15, 281.

[265] W. Lu, N. A. Lee, M. J. Buehler, *Proc. Natl. Acad. Sci. USA* **2023**, 120, 2305273120.

[266] B. Aaliya, K. V. Sunooj, M. Lackner, *Int. J. Biobased Plast.* **2021**, 3, 40.

[267] V. Yildirim, *Strojnícký časopis - J. Mech. Eng.* **2018**, 68, 33.

[268] J. W. Ponder, D. A. Case, *Adv. Protein Chem.* **2003**, 66, 27.

[269] O. T. Unke, S. Chmiela, H. E. Saucedo, M. Gastegger, I. Poltavsky, K. T. Schütt, A. Tkatchenko, K.-R. Müller, *Chem. Rev.* **2021**, 121, 10142.

[270] F. Schmid, *ACS Polym. Au* **2022**, 3, 28.

[271] A. Scacchi, M. Vuorte, M. Sammalkorpi, *Adv. Phys.: X* **2024**, 9, 2358196.

[272] H. Ji, W. Daughton, J. Jara-Almonte, A. Le, A. Stanier, J. Yoo, *Nat. Rev. Phys.* **2022**, 4, 263.

[273] A. Merchant, S. Batzner, S. S. Schoenholz, M. Aykol, G. Cheon, E. D. Cubuk, *Nature* **2023**, 624, 80.

[274] J. Jumper, R. Evans, A. Pritzel, T. Green, M. Figurnov, O. Ronneberger, K. Tunyasuvunakool, R. Bates, A. Zdek, A. Potapenko, A. Bridgland, C. Meyer, S. A. A. Kohl, A. J. Ballard, A. Cowie, B. Romera-Paredes, S. Nikolov, R. Jain, J. Adler, T. Back, S. Petersen, D. Reiman, E. Clancy, M. Zielinski, M. Steinegger, M. Pacholska, T. Berghammer, S. Bodenstein, D. Silver, O. Vinyals, A. W. Senior, K. Kavukcuoglu, P. Kohli, D. Hassabis, *Nature* **2021**, 596, 583.

[275] A. Patra, R. Batra, A. Chandrasekaran, C. Kim, T. D. Huan, R. Ramprasad, *Comput. Mater. Sci.* **2020**, 172, 109286.

[276] J. Abramson, J. Adler, J. Dunger, R. Evans, T. Green, A. Pritzel, O. Ronneberger, L. Willmore, A. J. Ballard, J. Bambrick, S. W. Bodenstein, D. A. Evans, C.-C. Hung, M. O'Neill, D. Reiman, K. Tunyasuvunakool, Z. Wu, A. Zemgulyte, E. Arvaniti, C. Beattie, O. Bertolli, A. Bridgland, A. Cherepanov, M. Congreve, A. I. Cowen-Rivers, A. Cowie, M. Figurnov, F. B. Fuchs, H. Gladman, R. Jain, et al., *Nature* **2024**, 630, 493.

[277] B. A. Morris, *The Science and Technology of Flexible Packaging: Multilayer Films From Resin and Process to End Use*, William Andrew, Norwich, NY, USA **2022**.

[278] S. Sutthasupa, M. Shiotsuki, F. Sanda, *Polymer Journal* **2010**, 42, 905.

[279] A. Das, T. Ringu, S. Ghosh, N. Pramanik, *Polym. Bull.* **2023**, 80, 7247.

[280] C. Li, L. X. Wang, *Chem. Rev.* **2018**, 118, 8359.

[281] OpenStax, Proteins, <https://bio.libretexts.org/@go/page/5309> (accessed: February 2025).

[282] OpenStax, Polysaccharides and Their Synthesis, <https://chem.libretexts.org/@go/page/36461> (accessed: February 2025).



Xing Quan Wang is a postdoctoral researcher in the Department of Mechanical Engineering at the University of California, Berkeley, specializing in AI-driven optimization of computational design and additive manufacturing processes. She earned her Ph.D. in Civil Engineering from City University of Hong Kong in 2022. Dr. Wang has made contributions to multiscale modeling, and computational mechanics of composite materials, leveraging AI-driven methodologies to bridge theoretical mechanics with practical applications. Her research emphasizes sustainability, advancing material behavior analysis and developing innovative computational techniques to support sustainable engineering and low-carbon solutions.



Zeqing Jin is currently a graduate student in the Department of Mechanical Engineering at the University of California, Berkeley. His research focuses on artificial intelligence-driven optimization of computational design and additive manufacturing process.



Dharneedar Ravichandran is currently a Postdoctoral Scholar at UC Berkeley. His work focuses on developing biopolymer-based composites for regenerative tissue engineering and advanced composite FEA models. Previously, he completed his Ph.D. in Manufacturing Engineering from Arizona State University, specializing in advanced materials and additive manufacturing. During his doctoral studies, Ravichandran made significant contributions to composite 3D printing techniques and nanoparticle-enhanced materials. His achievements include graduate research awards from AIChE, ACS, and ASME, and securing an NSF INTERN award. Ravichandran's expertise spans material characterization, process optimization, and interdisciplinary collaborations, with a focus on structure-morphology-process relationships.



Grace X. Gu is an Assistant Professor of Mechanical Engineering at the University of California, Berkeley. She received her Ph.D. and MS in Mechanical Engineering from the Massachusetts Institute of Technology and her BS in Mechanical Engineering from the University of Michigan, Ann Arbor. Her current research focuses on creating new materials with superior properties for mechanical, biological, and aerospace applications using multiphysics modeling and machine learning, as well as developing intelligent additive manufacturing technologies to realize complex material designs.